

NBSIR 81-2440

# Modeling of NBS Mattress Tests With the Harvard Mark V Fire Simulation

---

U.S. DEPARTMENT OF COMMERCE  
National Bureau of Standards  
National Engineering Laboratory  
Center for Fire Research  
Washington, DC 20234

Issued January 1982



QC  
100  
U56  
81-2440  
1982  
c. 2

---

DEPARTMENT OF COMMERCE  
NATIONAL BUREAU OF STANDARDS



FEB 24 1982

Not acc - Vic

QC100

U56

NO 71-5440

1982

C.2

NBSIR 81-2440

**MODELING OF NBS MATTRESS TESTS  
WITH THE HARVARD MARK V FIRE  
SIMULATION**

---

John A. Rockett

U.S. DEPARTMENT OF COMMERCE  
National Bureau of Standards  
National Engineering Laboratory  
Center for Fire Research  
Washington, DC 20234

January 1982

**U.S. DEPARTMENT OF COMMERCE, Malcolm Baldrige, *Secretary***  
**NATIONAL BUREAU OF STANDARDS, Ernest Ambler, *Director***



## TABLE OF CONTENTS

	Page
LIST OF TABLES . . . . .	iv
LIST OF FIGURES . . . . .	v
LIST OF SYMBOLS . . . . .	ix
Abstract . . . . .	1
1. INTRODUCTION . . . . .	1
2. GENERAL DISCUSSION OF THE HARVARD MODEL . . . . .	2
3. SECONDARY OBJECT SIMULATIONS . . . . .	4
4. INITIAL MATTRESS SIMULATIONS . . . . .	7
5. PROGRAM AND INPUT DATA CHANGES STIMULATED BY THE INITIAL SIMULATIONS . . . . .	9
6. SECOND SET OF MATTRESS SIMULATIONS . . . . .	13
7. ADDITIONAL MATTRESS SIMULATIONS . . . . .	16
8. ROOM "B" SIMULATIONS . . . . .	16
9. CONCLUSIONS . . . . .	18
10. REFERENCES . . . . .	20
APPENDIX I. The Effect of a Thin Char Layer on Pyrolysis Rate . . . . .	23
APPENDIX II. Hot-Cold Gas Mixing at the Vents . . . . .	25
APPENDIX III. Door Flows . . . . .	30
TABLES . . . . .	31
FIGURES . . . . .	33

LIST OF TABLES

	Page
Table 1. The computed effect of adjacent, connected rooms . . . . .	31
Table 2. The effect of a change of the smoke parameter, FS, mattress M01 . . . . .	32

LIST OF FIGURES

	Page
Figure 1. Burning rate versus time for 5 standardized wastebaskets. Also shown are the average burning rate versus time and the burning rate to be simulated . . . . .	33
Figure 2a. Calculated temperature versus time for the standardized wastebasket burned alone. Temperature and time scales are the same as will be used for mattress data . . . . .	34
Figure 2b. Mass loss rate versus time for wastebasket simulation. Vertical scale 12 X that used for mattress data . . . . .	34
Figure 3. Room upper gas temperature versus time for mattress M01 (data from [1, figure 17]). Also shown is the calculated hot layer temperature using Harvard default values except as noted in the text . . . . .	35
Figure 4. Room upper gas temperature versus time for mattress M05 (data from [1, figure 21]). Also shown is the calculated hot layer temperature using Harvard default values except as noted in the text . . . . .	36
Figure 5. Room upper gas temperature versus time for mattress M09 (data from [1, figure 25]). Also shown is the calculated hot layer temperature using Harvard default values except as noted in the text. The small hump at 450 seconds on the calculated temperature curve is caused by ignition and burning of the pillow. At this point the mattress burned, has terminated . . . . .	37
Figure 6. Room upper gas temperature versus time for control mattress (data from [1, figure 16]). Also shown is the calculated hot layer temperature default values except as noted in the text. The small hump at 500 seconds on the calculated temperature curve is caused by the pillow burning. At this point the bedding is burned out. This peak occurs slightly later than for the other mattresses due to the slower rate of growth of this relatively small fire . . . . .	38

LIST OF FIGURES (Continued)

	Page
Figure 7. Mass loss rate as a function of time for mattress M05 (data from [1, figure 13]). Also shown is the calculated mass loss rate using the Harvard default values except as noted in the text. The off-set of the two curves is not considered important, the difference in peak burning rate and rapid drop of the calculated curve are . . . . .	39
Figure 8. Semi-log plot of experimentally determined fuel mass and mass burning rate for mattress M05 (data from [1, figure 13] and numerical integration). Mass scale to the left, burning rate scale to the right . . . . .	40
Figure 9. Remaining fuel mass plotted against mass burning rate for mattress M05. Straight line corresponds to a "late burning constant" of 100 seconds (10 g/sec/kg fuel remaining) . . . . .	41
Figure 10. Remaining fuel mass plotted against mass burning rate for mattress M09. Straight line corresponds to a "late burning constant" of 100 seconds (10 g/sec/kg fuel remaining) . . . . .	42
Figure 11. Remaining fuel mass plotted against mass burning rate for mattress M02. Straight line corresponds to a "late burning constant" of 100 seconds (10 g/sec/kg fuel remaining) . . . . .	43
Figure 12. Location of "Room A" within the NBS Fire Test Building showing its relation to other, connecting rooms and the fire gas exhaust system . . . . .	44
Figure 13. Upper gas temperature versus time for mattress M01 (data from [1, figure 17]). Also shown is the calculated hot layer temperature using default values except as noted in the text. Simulation includes door mixing . . . . .	45
Figure 14. Height versus room temperature for mattress M01 (data from [1, figure 23]). Also shown are the calculated vertical distribution with and without door mixing and for the door opening narrowed to 71 percent of its actual width . . . . .	46



LIST OF FIGURES (Continued)

	Page
Figure 15. Upper gas temperature versus time for mattress M05 (data from [1, figure 21]). Also shown is the calculated hot layer temperature with door mixing using Harvard default values except as noted in the text . . . . .	47
Figure 16. Upper gas temperature versus time for mattress M09 (data from [1, figure 25]). Also shown is the calculated hot layer temperature with door mixing using Harvard default values except as noted in the text . . . . .	48
Figure 17. Upper gas temperature versus time for control mattress (data from [1, figure 16]). Also shown is the calculated hot layer temperature door mixing using Harvard default values except as noted in the text. The small hump at 430 seconds on the calculated temperature curve is caused by the pillow burning. At this point the bedding is burned out . . . . .	49
Figure 18. Height versus room temperature for mattress M05 (data from [1, figure 32]). Also shown are the calculated vertical distribution with door mixing and door narrowed to 71% of actual width . . .	50
Figure 19. Mass loss rate as a function of time for mattress M05 (data from [1, figure 13]). Also shown is the calculated mass loss rate using the Harvard default values except as noted in the text. The offset of the two curves is not considered important . . . . .	51
Figure 20. Extinction coefficient computed from light attenuation measurements taken in the doorway, 0.61 m below the ceiling, room A, mattress M05. Also shown is the computed extinction coefficient for the upper gas layer with $FS = 0.241$ . . .	52
Figure 21. Comparison of measured and calculated heat flux at a target separate from the fire, mattress M05. Experimental data from [1, figure 43] . . . . .	53
Figure 22. Effect of fire-target spacing on heat flux to the target, computed for mattress M05 at time of peak burning . . . . .	54

LIST OF FIGURES (Continued)

	Page
Figure 23. Upper gas temperature versus time for mattress M02 (data from [1, figure 18]). Also shown is the calculated hot layer temperature with door mixing using Harvard Code default values except as noted in the text . . . . .	55
Figure 24. Upper gas temperature versus time for mattress M04 (data from [1, figure 20]). Also shown is the calculated hot layer temperature with door mixing using Harvard default values except as noted in the text . . . . .	56
Figure 25. Upper gas temperature versus time for mattress M06 (data from [1, figure 22]). Also shown is the calculated hot layer temperature with door mixing using Harvard default values except as noted in the text . . . . .	57
Figure 26. Room B (ventilated) upper gas temperature for mattress M05, data from [1, figure 21] and values computed with the room door fully open and closed to several widths . . . . .	58
Figure 27. Room B (un-ventilated, augmented area) upper gas temperature for mattress M05, data from [1, figure 21] and values computed with the room door closed to 0.2 m width . . . . .	59
Figure 28. Calculated height of the lower surface of the hot gas layer for several cases, room B and room B (augmented). Note that the layer descends much more rapidly for the smaller area (actual) room B as compared to the augmented room . . . . .	60
Figure A2.1 Room radiative heat flux calculation showing the equations to be solved and the geometric relation of the terms . . . . .	61
Figure A3.1 Door mass outflow rate as a function of heat release rate. Points from Steckler [A3.1], curve calculated . . . . .	62
Figure A3.2 Door mass outflow rate as a function of door width. Points from Steckler [A3.1], curve calculated . . . . .	63

## LIST OF SYMBOLS

$A_c$	cool layer surface area, $m^2$
$A_H$	hot layer surface area, $m^2$
$A_{vt}$	total area of that part of the vents above the hot-cool gas interface, $m^2$
C	orifice flow coefficient = 0.68
D	height of the hot-cool interface in the room, m
d	char thickness, m
e	emissivity
	subscripts: C cool gas layer
	F floor and lower walls
	H hot gas layer
	W ceiling and upper walls
FL1	radiant flux exchanged between the hot layer and the ceiling, $W/m^2$
FL2	radiant flux exchanged between the hot and cool layers, $W/m^2$
FL3	radiant flux exchanged between the cool layer and the floor, $W/m^2$
FS	mass of smoke produced per unit mass of fuel pyrolyzed
FSINIT	value of FS for fuel burned in ambient air
f	dimensionless factor in burning rate expression, defined in section 5 of the main text
g	acceleration of gravity, $m/s^2$
h	height above fuel surface of apparent flame radiation source, m
I	radiant flux, $W/m^2$
	subscripts: 1 - upward flux in hot layer
	2 - downward flux in hot layer
	3 - upward flux in cool layer
	4 - downward flux in cool layer
K	coefficient = 1/2 used in door mixing correlation [15]
k	dimensionless constant, section 5, main text
k	extinction coefficient, $m^{-1}$
k	char thermal conductivity, appendix I, $W/mK$
m	fuel mass, kg
$\dot{m}_i$	mass flow rate in through the lower part of a vent, $kg/s$

LIST OF SYMBOLS (Continued)

$\dot{m}_m$	mass transfer rate from hot to cool layer by mixing, kg/s
$\dot{m}$	mass burning rate, kg/s
$\dot{m}_p$	mass burning rate calculated from heat flux incident on fuel, kg/s
N	height of the neutral plain in the doorway, m
n	exponent
R	= $9/(8C Ri)$ , used in appendix II
Ri	Richardson number
r	dimensionless constant
r	radius, m
	subscripts: F radius of fire
	L "radius" of hot-cool gas layer interface
	S radius of fuel surface
STOIC1	value of XGAMMA for ambient air
STOIC2	value of XGAMAS for ambient air
T	temperature, K
	subscripts: A ambient air
	C cool gas layer
	F floor
	H hot gas layer
	W ceiling
TECPR	flame radiation incident on the cool layer, $W/m^2$
TECZR	radiant energy gain by the cool layer
TEPZR	total flame radiation
$t_o$	characteristic time, s
$u_i$	velocity of gas entering room, m/s
V	layer volume, $m^3$
W	width of room wall containing door, m
Wo	width of door, m
WL	area of interface between hot and cool gas layers, $m^2$
XGAMMA	grams of air which must be entrained by a buoyant fire plume to burn a gram of fuel
XGAMAS	stoichiometric air/fuel ratio

LIST OF SYMBOLS (Continued)

x	$4R/(9 + 4R)$ dummy variable used in Appendix II
z	= 4 kV/A used in Table 2
ZUFI	value of ZUFZZ for ambient air
ZUFZZ	extinction coefficient for flame, $m^{-1}$
ZYCO	mass fraction of oxygen in the cool, lower gas layer

Greek letters

$\sigma$	Stephan-Boltzman constant
$\rho_L$	density of gas in the hot layer
$\rho_o$	density of ambient air





# MODELING OF NBS MATTRESS TESTS WITH THE HARVARD FIRE CODE

John A. Rockett

## Abstract

NBS burned eleven mattresses made up with bedding in two different rooms, typical of a residential bedroom and a nursing home patient room, respectively. Seven of the mattresses flamed and burned vigorously, the other four were of a construction or so heavily flame inhibited that they only smoldered. The burning behavior of the seven that flamed was modeled with the Harvard mark V fire simulation. The experimental burn behavior for tests conducted in one room was well reproduced using only total weight of combustible, surface area and heat of combustion. Smoke production values were found to have little effect on the predicted behavior except for the smoke production itself. Fires in a second room, whose ventilation was intentionally restricted by the configuration of the adjoining space, could not be as well reproduced by the present, single room fire model.

During this study several changes were made to the simulation. The most significant change was the inclusion of mixing of the hot, exiting fire gases with the cold incoming air. As a part of this, the inter-layer radiation exchange was reformulated to include the effect of smoke contamination of the lower layer. The reformulation of the radiation model had a marked effect on the predicted upper layer gas temperatures, generally improving the quality of the simulation.

## 1. INTRODUCTION

Over a period of several years, beginning in mid 1976, NBS conducted a number of tests involving mattresses. These included burning complete beds in a room [1], and testing of samples cut from mattresses in "bench-scale tests" [2]. During this same period, Harvard University had been developing, under a series of grants from NBS, an analytic room fire simulation [3-6]. A major input to the development of this simulation was a series of full scale bedroom fires conducted by the Factory Mutual Research Corporation between 1973 and 1975 [7-9]. The fires used by Harvard for testing the operation of the simulation have been these or other, more idealized bed-like fires burned at Factory Mutual as a part of the same program. This report compares the results from running the Harvard simulation in various configurations with the corresponding NBS full scale test results.

## 2. GENERAL DISCUSSION OF THE HARVARD SIMULATION

The Harvard Fire Simulations used for this study were interim versions issued to NBS during 1980-1981 and designated as H04 and H05. A version, designated H05.1, was an NBS modification of H05. The simulation represents fire in a single room with vents opening directly to an infinite plenum. The program requires that initial values for a number of variables be set. For all of these, values are provided internally by the program. However, any of these can be altered by the user at his discretion through the input routines. In default of the user making a change, the preset value is used. Following common computer terminology, the unaltered, preset values are referred to in this paper as "default values". The input routines allow for entering the following room data:

### Geometric:

Length	m
Width	m
Height	m
Number of Objects	

### Vents:

Number of Vents (for each vent)	
Width	m
Height	m
Transom Depth	m

### Walls:

Thickness	m
Thermal Conductivity	W/m °C
Specific Heat	J/kg °C
Density	kg/m <sup>3</sup>

### Other:

Ambient Temperature	K
---------------------	---

All these data were available for both rooms in reference [1] and the values appropriate to the NBS rooms were used.

The full-scale NBS tests to be simulated were conducted in two different rooms. Room A was 3.4 m wide, 3.5 m deep and 2.44 m high. It was ventilated by a single opening, a door 0.91 m wide by 2.13 m high (door transom 0.31 m deep). Room B was 4.22 m wide, 3.35 m deep and 2.44 m high with a single door 1.07 m wide by 2.03 m high (door transom 0.41 m deep). The walls and ceilings were cement-asbestos board [1, p. 11].



The Harvard fire simulation allows up to five objects per room with the possibility of one object igniting another. In the simulation as received, level 4's, the only mechanism for secondary ignition was by radiant heat. A simple change, now incorporated as a standard feature of the simulation, allows ignition of contiguous objects by flame spread.

The fire simulation allows entering the following data for each object:

Geometric:

(coordinates relative to the front, left, lower room corner)

x coordinate of object center	m
y coordinate of object center	m
z height of object top surface	m
Thickness	m
Initial burning radius	m
Maximum burning radius	m

Thermal:

Initially ignited or not	
Type of fire:	gas burner pool growing special
Effective air/fuel ratio	default value 14.45
Stoichiometric mass ratio	9.85
Specific heat	19.00 J/kg K
Density	48 kg/m <sup>3</sup>
Surface emissivity	0.98
Fraction of heat of combustion actually released	0.65
Heat of combustion	2.87x10 <sup>7</sup> J/kg
Heat of vaporization	2.05x10 <sup>6</sup> J/kg
Initial fuel mass	6.852 kg
Temperature at ignition	727 K
Temperature at onset of pyrolysis	600 K
CO <sub>2</sub> mass evolved/fuel mass burned	1.504
CO mass evolved/fuel mass burned	0.013
Smoke mass evolved/fuel mass burned	0.241
HO mass evolved/fuel mass burned	0.714
Flame spread parameter	0.0109

For all of these, the default values built into the simulation are based on the polyurethane mattresses burned in the Home Fire Project room burns [7-9]. Several of these data elements require explanation:

1. In the simulation, all objects burn as circular fires. A growing fire starts at the center of the object with the given, initial radius. The fire radius increases with a velocity that is related to the heat flux incident on the fuel surface and is a linear function of the flame spread parameter, until it reaches the specified maximum radius [5]. The maximum fire radius is chosen to yield a

burn area equal to the actual maximum burning area for the fully involved object, regardless of its shape. The mass burning rate per unit area depends on the heat flux incident on the fuel.

2. The stoichiometric mass ratio (default value 9.85) depends on the fuel chemistry and is the mass of air needed to fully burn a unit mass of fuel under ideal conditions. The effective air/fuel ratio (default value 14.45) is the amount of air which must be entrained by a buoyant diffusion fire plume to burn (as fully as possible in such a flame) a unit mass of fuel. This exceeds the stoichiometric mass ratio because, due to the poor mixing in the turbulent plume, quite a bit of the air entrained never comes in contact with fuel. Complete combustion is seldom approached in diffusion flames. The degree of completeness is represented through the fraction of heat of combustion actually released (default value 0.65).

The Harvard simulation, as received, provided algorithms for three types of fire, all assume a smooth, horizontal fuel surface: (1) A gas burner. For this the burning rate is set by the gas flow rate, specified as input in addition to the above list. (Other, nominal input items not applicable to a gas burner are ignored.) (2) A pool fire. This is a fire of fixed area, whose burning rate is set by the heat flux reaching the fuel surface. (3) A growing fire. This is a fire whose area is a function of time and whose burning rate per unit area is set by the heat flux reaching the fuel surface. For both growing and pool fires, the fuel pyrolyses at a fixed temperature with a prescribed latent heat of vaporization. Burning stops when all the fuel is exhausted. To prevent numerical problems and better simulate actual burning behavior, burn-out does not occur abruptly but is smoothed over a short time. The time interval for burn-out is built into the algorithms.

In principal, if the burning behavior of the object to be simulated will not be well represented by one of these three fire types, a special algorithm for that object should be supplied. Another modification introduced to the NBS versions of the Harvard simulations was the provision of a mechanism for calling for a fourth fire type, a Special Fire. With this option the individual user is free to construct his own burn algorithm as needed. This will be discussed later.

### 3. SECONDARY OBJECT SIMULATIONS

The simulations were to include several objects in the test rooms. For each test, the rooms were furnished with a bed and wastebasket. The wastebasket was polyethylene, 282 g weight, 248 mm x 178 mm x 254 mm high filled with a "standardized" fuel weighing 443 g for a total weight of 725 g [1, table 6]. The bed was a steel frame with an open wire grid on which the mattress and bedding to be tested were placed. The mattress itself varied from test to test but each was "made up" with an identical covering consisting of a cotton drawsheet, 2 50-50 cotton-polyester blend

sheets, and an 86 percent cotton, 14 percent polyester spread. These covers weighed 2.67 kg. At the head of the bed was a single polyurethane pillow with cotton cover, polyvinyl chloride protector and 50-50 cotton-polyester pillow case. The pillow and its covers weighed 1.04 kg [1, table 5].

Figure 1 shows the result of burning five of the "standard wastebaskets", two burned by Babrauskas at University of California, Berkeley, and three at NBS [10].\* Also included on figure 1 are the average burning rates at each of the nine times when data was recorded. The numerical simulation of the wastebasket would have a more regular behavior. This was selected by a further smoothing of the averaged experimental data and is also shown on the figure. Note that the peak burning rate of 1.64 g/s and integrated fuel consumption results in only 350 g burned. Babrauskas indicated that the wastebaskets were not fully consumed, but left a substantial residue of sticky char [11]. The fuel weight used for the simulation, 350 g, rather than 725 g, is consistent with the behavior illustrated in figure 1 and is believed to represent the situation more correctly. Note that this average behavior, which was arrived at from somewhat sketchy data prior to publication of [10], is slightly different from that found by analysis of more complete data.

A wastebasket fire would not fall naturally into one of the three fire types for which algorithms are supplied. However, it was possible to find a set of input parameters for a growing fire which produced the desired effect. Since modeling wastebasket fires was not a major objective of this study, the somewhat artificial parameters needed to accomplish this were not considered significant. The non-default values used were:

Geometric:

x	3.21	m
y	1.65	m
z	0.254	m
Thickness	0.25	m
Maximum Radius	0.1185	m

Thermal:

Density	35	kg/m <sup>3</sup>
Heat of Vap.	4.0510 <sup>5</sup>	J/g
Initial Mass	0.35	kg

---

\*The fire load in the Berkeley wastebaskets was not quite the same as in the mattress tests.

Figure 2 shows the calculated temperature history for the wastebasket burned alone. The mass loss rate rises rapidly and, at 50 seconds, stabilizes at a constant value. It remains at this value until 240 seconds after which the mass loss rate drops rapidly. The available fuel is exhausted at 270 seconds. This reproduces quite closely the smoothed, average behavior illustrated on figure 1.

The wastebasket location was chosen to cause ignition of the bedding 30-40 seconds after the wastebasket ignited. The y and z values given above were varied slightly to give consistent ignition times for the various size and thickness mattresses.

It was reasonable to expect the pillow to be simulated fairly well by the growing fire algorithm. Its location was at the "head of the bed". The following non-default values were used for the initial simulations.

Geometric:

x	2.64	m
y	3.035	m
z	0.76	m
Thickness	0.15	m
Maximum radius	0.488	m

Thermal:

Density	19.32	$\text{kg/m}^3$
Heat of combustion	$2.15 \times 10^7$	J/kg
Initial mass	1.04	kg
Fire spread parameter	$0.2541 \times 10^{-2}$	

In addition to the wastebasket, the pillow and the mattress, one other object was placed in the room. The purpose of this was to force the program to calculate and tabulate the heat flux at this object. Its burning behavior was not considered; its ignition temperature was set sufficiently high that it would never ignite. This object was positioned to record the heat flux near the door. It was located at:

Geometric:

x	2.16	m
y	0.01	m
z	0.75	m

For a few cases, to be discussed separately this target object was moved to other locations.

It should be pointed out that inclusion of this target object occasionally caused convergence problems late in the fire, after most or all the fuel had burned out. It has not yet been conclusively determined why this happens. More often than not the problem didn't arise, making its diagnosis more difficult. To complete the calculation to the desired final time, when these troubles occurred, the target (fourth) object was



removed and the case re-run. This usually worked. Problems also arose early in the calculation from time to time. These did not seem to be related to the fourth object. These problems could be eliminated by a seemingly trivial change, usually in location of one of the secondary objects (wastebasket location changed a few millimeters--which changed bedding ignition time a second or two, or the pillow--which changed its ignition time slightly).

#### 4. INITIAL MATTRESS SIMULATIONS

The mattresses tested are designated as M01 through M10 in reference [1]. The same notation is used here. Three of the mattresses were basically polyurethane foam construction, M01, M05, and M09 [1, table 8]. They differed in details of construction, type and amount of flame retardants, and total weight of combustible material. Nevertheless, they might be expected to burn in a manner similar to those tested by Factory Mutual. Accordingly, initial runs were made to simulate the burning of these three mattresses using the program default values for all the mattress variables except location, size, weight and heat of combustion. The weights used were those given in [1, table 10]. They were increased, in each case, by 2.67 kg to account for the bedding. The heat of combustion values used were weight averaged for the bedding and mattress materials. The cotton-polyester value from reference [2, table 10], 21.2 MJ/kg was used for the bedding and the total heat value from reference [2, table 11] for the mattress. The fraction of this heat actually released,  $\chi$ , was taken from reference [2, table 11], again for the mattress in question. One additional run was made in this series to simulate the burning of the "Control" mattress, an inert fiberglass bun (no combustible binder in the fiberglass) covered with the standard bedding (designated as MOC).

The values used for all the mattresses were:

Geometric:

x	2.64	m
y	2.28	m
z	0.61	m
Maximum Radius	(see discussion below)	

The maximum radius chosen for mattresses M01 and 5 corresponds to twin size mattresses. M09 was cot size and a smaller radius was used. Note, however, that M01 and 5 were not exactly the same size. The maximum radius and thickness were varied in accordance with these small differences in size. The result, except for M09, was probably not significantly different than would have been found by using the same values for all the mattresses. The "Control" mattress had the same area as was used for M05; its thickness was taken to be that of the bedding alone, 0.0033 m. The values used were:

Thermal:			
<u>Initial Mass</u>	<u>Heat of Comb.</u>	<u><math>\chi</math></u>	<u>Effec. Heat of Comb.</u>
M01 16.27 kg	28.2 MJ/kg	0.84	23.7
M05 8.57 kg	26.7 MJ/kg	0.79	21.1
M09 5.87 kg	25.8 MJ/kg	0.74	19.1
M00 2.67 kg	21.2 MJ/kg	0.74	15.7

Note that the effective heats of combustion (heat of combustion times  $\chi$ ) vary only about 20 percent from the average for these three mattresses while the total mass of combustible varies by almost a factor of three from the lightest to the heaviest mattress. Thus, this first set of simulations mainly demonstrate the effect of varying the amount of combustible on the bed. It should also be born in mind that, although these mattresses varied in type and amount of flame retardant, we do not, currently, have any technically sound method for simulating the effect of retardants. All these mattresses burn alike as far as the simulation is concerned.

The first simulations used the standard growing fire algorithm and did not include mixing of the upper and lower gas layers at the door. The results of these simulations are compared with the test values in figures 3-6. In all these figures, the temperature of the gas near the room ceiling has been compared with the simulation's upper layer temperature, a single average temperature for the gas in the entire upper part of the room. Note first, that the computed temperature (up to 200 seconds) is controlled by the wastebasket, although the bedding ignites in each case at about 35 seconds. Note also that in each case the simulation shows a rapid temperature rise at about 300 seconds as the bedding and mattress become the dominant source of heat. The experimental and computed time for rapid temperature rise are quite similar for M01. But for M05 and M09 the experimental temperature rise occurred quite a bit later than for the simulation. The simulation of the control, M0C, figure 6, appears qualitatively different than the test. Referring to the text and figures in reference [1], from which the data used here were taken, we see that there was generally quite a lot of variation from test to test with nominally similar mattresses, especially in the time when rapid temperature rise occurred. Babrauskas [11] attributed this to variations in the way in which the bedding became involved. He also said that the bedding seemed to control the rate of development of the fire while the mattress determined the severity of the fire. In our simulations there is, of course, consistency in the way in which the fire develops. Throughout this study differences in the time to reach maximum upper gas temperature were found for the simulation as compared to the test data. This difference was not considered significant in view of the scatter in the experimental data in time to reach peak temperature. The value of the peak temperature was, however, quite reproducible between tests and was considered important to assessment of the quality of the simulation.

## 5. PROGRAM AND INPUT DATA CHANGES STIMULATED BY THE INITIAL SIMULATIONS

These results were only moderately encouraging, and, on looking more closely, definite problems appear. Figure 7 compares the experimental and calculated rate of mass loss for mattress M05. It was typical of all four of this first group of simulations. The peak mass loss rate was more than twice the experimental value and the burn-out, after the peak mass loss rate occurs, is far too rapid. With this high maximum burning rate, it is not surprising that the peak calculated temperatures exceed the experimental values; for M01, the lower calculated maximum temperature arises for a different reason which will be discussed later. There are several reasons that the simulation might find too large a peak burning rate. First, the heat of pyrolysis could be wrong, since burning rate is directly proportional to heat of pyrolysis. For heat of pyrolysis alone to account for the high burning rates, it would have to be off by a factor of about 2. Because no measured values were available for these mattresses, the default values were used. It seems highly unlikely that this could differ so much from the actual values. Second, burning area could be wrong. The Harvard simulation assumes that the fire grows as a circle until limited by the (input) maximum burning area. Burning then continues at that area until all the fuel is exhausted. But the mattresses are relatively thin fuels. Before burning has stopped in one location, complete burn-through may have occurred at another location where the fire has been burning longer. This would be especially true for the bedding. The idea was explored using a special fire algorithm built by modifying the standard growing fire algorithm. The new routine provided for both a circular, growing fire and also a central, circular non-burning region which grew as the fuel became locally exhausted. This produced some effect on peak burning rate, but not nearly enough to account for the discrepancy. Furthermore, it had almost no effect on the too rapid drop in burning rate after the peak occurred. The slow decay of the fire could possibly also be simulated by accounting for the effect of a circular fire burning on a rectangular bed. After the centrally located fire radius reached the smaller dimension of the bed, two circular arc fires would remain, the arc length decreasing with further growth. When the radius reached the larger dimension, only four small fires would remain. The arc lengths of these would also decrease with time. This was simulated though the algebra became somewhat complex. It helped but not enough. As a part of this algorithm, provision was made for two fuel layers, one, to be the bedding, lying on top of the other, the mattress itself. The fire parameters of these two layers were entered separately. Thus the same bedding data could be used for all mattresses. In this way fire growth was controlled by the bedding parameters alone but, since peak burning occurred after most or all of the bedding layer had been burned off, peak burning rate was controlled by the mattress parameters. Finally, the rate of pyrolysis would be wrong if the amount of heat reaching the virgin fuel were wrong.



Because of the known presence of retardants in some of the mattresses, and because it has been observed that flame retardants tend to increase char at the expense of volatiles, it seemed worthwhile to explore the possibility that the burning behavior, late in the fire, was modified as a result of char formation. Accordingly, the laminated fuel algorithm was further modified to include the effect of an inert char layer, formed as the fuel was burned. The char layer impeded the flow of heat into the fuel and its increased surface temperature increased radiation losses from the fuel. Appendix I gives a numerical example of the effect of an idealized, inert char layer such as might be simulated by the empirical changes detailed here. It shows that, to produce the observed effects, i.e., a decrease in burning rate of mattress M05 from 118 to 46 g/sec, a homogeneous char layer would be very thin (about 1/2 mm). So thin a layer is seldom homogeneous and more complex geometries are awkward to model. Implicit in using char to explain the burning rate behavior is the assumption that the char formation (or burning surface area) is somehow related to the fuel mass remaining. This algorithm has a fairly sound physical foundation, but had become quite complex and required additional parameters as input for which there were no data. Thus in practice, its use was quite empirical. It must be remembered, too, that the growing fire algorithm, from which it derived, is essentially an empirical correlation of experimental data. A much simpler and just as logical approach would be to alter the original empirical correlation.

Figure 8 is a semi-log plot of experimental data for mattress M05. One curve gives the fuel mass (left scale) versus time and the other mass burning rate (right scale) versus time. In figure 9 this data is replotted with fuel mass plotted against mass burning rate. Note that, after the peak burning rate has occurred, burning rate becomes roughly proportional to fuel mass remaining. In this example the constant of proportionality is 10 g/sec/kg fuel remaining. (Straight line on fig. 9). Figures 10 and 11 show similar plots for two other mattresses, one, M09, has a urethane core and the other, M02, is an inner spring construction whose principal combustible is polyurethane padding. They do not show quite as "clean" a trend as figure 9, but they are generally consistent with it. Now, for quite another reason--to avoid numerical problems with a too abrupt fuel burn-out--Harvard simulation has instructions which accomplish precisely this burning rate behavior. The standard growing fire algorithm (and pool fire too) include a relation which "adjusts" the pyrolysis rate according to:

$$\dot{m} = \dot{m}_p (1 - \exp(-m/t_o \dot{m}_p))$$

where

$\dot{m}$  = the adjusted pyrolysis rate

$\dot{m}_p$  = pyrolysis rate computed from (non charring) fuel properties and energy flux to the fuel surface

$m$  = remaining fuel mass

$t_o$  = a time constant set equal to 2 sec. by Mitler



When  $m$  is large and  $\dot{m}_p t_o$  small,  $\dot{m} = \dot{m}_p$ , but near burn-out,  $m$  becomes small and this expression approaches

$$\dot{m} = m/t_o.$$

Thus, the observed behavior of mattress M05 could be represented by changing  $t_o$  from 2 seconds to 100 seconds. To test this idea a new special fire algorithm was set up which differed from the standard growing fire only by making  $t_o$  an input parameter. After a few preliminary trials, a further change was made to decouple the time,  $t_o$ , at which the shift (from energy flux determined pyrolysis to mass remaining determined pyrolysis) occurred and the proportionality constant applicable after the shift. This was done by setting

$$f = m/t_o \dot{m}_p$$

$$k = 1 - (1 - r)\tanh(1/f)$$

$$\dot{m} = \dot{m}_p k(1 - \exp(-f))$$

Note that when  $f$  is large  $k = 1$  and  $\dot{m} = \dot{m}_p$ , but when  $f$  is small  $k = r$  and  $\dot{m} = \dot{m}_p r f = m r / t_o$ . The next set of simulations presented here were run with  $t_o = 40$  sec. and  $r = 1/2$  (equivalent to a late fire burning constant of 80 sec., somewhat less than the M05 indicated value of 100 sec.\*).

Experiments by Kashiwagi [12] provide an alternative explanation for the Harvard code's over estimation of pyrolysis rate. His data suggest that a substantial fraction of the flame radiation directed toward the fuel is absorbed by cool fuel vapor just above the surface. If 60 percent were absorbed, the calculated and observed pyrolysis rates for mattress M05 would agree. Mitler had partially compensated for this effect by his choice of flame temperature (somewhat lower than that measured by Orloff [13]) in early versions of the Harvard code. The more recent versions, including level five, use an average flame temperature of 1260 K which agrees with Orloff but the simulation does not include radiation blockage. However, while radiation blockage is certainly present and is probably of about the right order of magnitude, it would not, alone, give the observed dependence of burning rate on mass remaining late in the fire. In any event, we do not yet have available any data on radiation absorption coefficient for raw fuel at pyrolysis temperatures, nor a satisfactory model for the radiation blockage so, again, an empirical approach is indicated for the present.

The empirical approach seems a simple way around a difficulty. It does not, however, provide guidance in predicting burning behavior of char-forming materials of a distinctly different class.

---

\*80 seconds was chosen after a somewhat less careful study of the data than that shown in figures 8-11 but, having started with 80 seconds, it was retained. As will be seen later, 100 seconds might have been better.

The above discussion deals with the too high burning rate. This was found for all the first set of simulations, but not all produced too high an upper gas temperature. For M01, although the peak temperature pyrolysis rate was high, the peak temperature was too low. Examination of figures 27-36 of reference [1] showed that, for all the mattresses which burned vigorously, the gas temperature in the lower part of the room was well above ambient. This kind of behavior has often been found and is attributed to mixing of the outflowing, hot combustion products with inflowing cool air close around the vents [14-16]. From reference [1, figures 27-36] it is apparent that considerable mixing may have occurred (at the room door) between the hot combustion products leaving and the cold incoming air. This is most obvious for the larger fires, for example M01. The Harvard simulation, level five and earlier, does not include this effect. Because mixing seemed important, changes were made to add mixing of the exiting and entering flows at the door. Mixing results not only in heating of the air in the lower part of the room but also its contamination with combustion products. When mixing is large, this can result in a significant radiant energy exchange between the upper hot layer and the lower warm layer. This effect was also included. A more detailed description of these changes is given in appendix II. The door mixing modified simulation is referred to as H051.

The room geometry shown in [1] is not strictly correct for room A. The room itself is shown correctly, but its door did not open directly to a large exhaust plenum as might possibly be inferred. Rather it connected to another room which, in turn, exhausted into a 21 foot long corridor connecting to the exhaust hood. The complete geometry is shown in figure 12, taken from King-Mon Tu [17]. Although he concluded that the effect of the adjoining rooms was small, the state of knowledge at the time he made his measurements would not necessarily have led to detection of some effects.

To estimate the effect of the complete room-corridor system vis-a-vis an isolated room, Tanaka's multi-room fire simulation [18] was run for two pairs of cases: room A by itself and room A plus its adjoining room and corridor, each for two different fire sizes. Tanaka's plume model, which is valid for small area fires (his primary concern), under-estimates the entrainment for large area fires. The plume algorithm was changed slightly to correspond to that used in the Harvard simulation\*. The results of the two pairs of calculations are summarized in table 1. Note that the flow for the complete room-corridor system was about 75 percent of the flow for the isolated room.

---

\*This raised the question of which plume model was the better. A partial answer is provided in appendix III.

To simulate the effect of the adjoining room and corridor on the fire behavior as computed by the Harvard simulation, the room door was made narrower. The amount of narrowing to be used was based on the following rather intuitive idea: Since the two doors between the fire room and the vent (see fig. 12) were the same size, a uni-directional flow would produce equal pressure drop across each door. Removing one door, without changing the total pressure difference available, would cause the flow to increase as the square root of the pressure drop across one door, now double its previous value. Thus, to reduce the flow to its previous value, the door area should be reduced to 70.7 percent of its original value. This area reduction was accomplished by narrowing the door without changing its height. The result of this 70.7 percent change and also a change to 50 percent of the actual door width are summarized at the bottom of table 1. Note that, for the 70.7 percent door, the flow change is quite close to that predicted by Tanaka's model. In all the remaining room A simulations to be discussed the door width was 0.643 m, 70.7 percent of the actual width.

One further change was made at this point. Babrauskas pointed out [11] that, in the Harvard simulation, the heat released in the plume is the product of the fuel mass loss rate times the heat of combustion, adjusted to ambient temperature, but based on fuel supplied in a gaseous state. Some of the energy released in the plume is radiated away and a fraction of this is used to pyrolyze the fuel. The heats of combustion given in [2, tables 10 and 11] assume the fuel is present as a solid. Thus the heats of combustion taken from these tables should be increased by the heat of pyrolysis for use with the Harvard model. This represents about a 7 percent increase in the heat of combustion. Further, experience with the laminated fuel model, discussed above, had shown that most of the bedding had burned off prior to the time of peak burning. Accordingly, the weight averaged heat of combustion was no longer used, rather the mattress values from [2, table 11] were used. To make the values consistent with the Harvard usage, these were increased by adding to them the Harvard default value for the heat of pyrolysis.

## 6. SECOND SET OF MATTRESS SIMULATIONS

After making the program and input data changes discussed above, a second set of calculations were made. Figure 13 shows the temperature-time comparison for the H051 simulation corresponding to the simulation shown in figure 3. The peak temperature was still low, but, in this case, the peak burning for mattress M01, which had been 146 g/sec., was now 97.32 g/sec. The drop in temperature after the peak, which had been too abrupt, was now slower. Figure 14 shows a comparison of the vertical temperature distribution as measured at three locations away from the bed and calculated with and without mixing. Note that the lower gas temperature had risen much more than the upper. This is due to the rapid increase with temperature of radiation loss from the hot layer. Without burning in the upper layer, another effect that the present fire code does not include, it may be difficult to match the upper gas temperature, although the method



of calculating radiative exchanges is also very important (see appendix II). Figures 15-17 are temperature comparisons similar to figure 4-6. There is a smaller effect of door mixing for these fires, see figure 18. Figure 19 is similar to 7 and shows that the peak burning rate for M05 is now about correct. Except for M01, these results are quite encouraging.

The low peak temperature as simulated for M01 could be related to the choice of the parameters which determine the hot layer emissivity. Up to this point the Harvard values had been used. With these, the extinction coefficient calculated for M01 at peak burning is  $7.35 \text{ m}^{-1}$ . Babrauskas [1] found values of  $3-5 \text{ m}^{-1}$  based on smoke measurements in the room. Tewarson [19] reports various values for flexible urethanes suggesting values for the Harvard input smoke parameter, FS, from as large as that used by Harvard ( $0.241 \text{ g smoke/g fuel pyrolyzed}$ ) to  $1/3$  that value. The extinction coefficient found by Babrauskas suggested cutting the smoke parameter, FS, roughly in half; the new value would still be consistent with Tewarson's data. The calculated effect was small. In view of the known importance of radiation in room fires this was rather surprising.

Table 2 shows heat balances for M01 at peak burning for two values of the smoke parameter. Note first that, because Mitler uses a variable beam length, [5, page 38], for heavy smoke, reducing the extinction coefficient does not reduce the emissivity very much. Halving the smoke produced changed the emissivity from 0.98 to 0.95. Thus the layer is quite black for both rates of smoke production.

By far the biggest elements in the heat balance are the terms expressing the energy convected through the hot layer. Almost exactly half the energy released by the fire passes directly out the door. It is the disposition of the remaining half that concerns us, but the large energy "flushing" that accompanies this must always be kept in mind. The difference between the energy added by convection from the fire plumes and that removed out the door, and by convective mixing around the door, is the net convective energy. While large, this does not completely dominate the other terms. The net convective energy changes only slightly with the change in smoke density--down 17 kW or 2 percent.

The largest change shown in table 2 is in the heat lost to the lower layer--down from 770 to 689 kW, a reduction of 81 kW or 11 percent. The next largest change is in the radiant heat from the flames absorbed by the hot layer. This is reduced 31 kW or 6 percent. These two effects are in the direction to be expected with the reduced layer emissivity. Because the decrease in heat loss from the layer is more than the decrease in the heat gain from the flames, the net effect is that, for the less smoky case, the layer should be a bit hotter.

The third largest change is in the radiant heat lost to the ceiling, which increased 23 kW or 7 percent. The decreased layer emissivity results in a lower ceiling temperature. The radiation term in table 2 relating to the ceiling is the net radiative exchange. It is the difference between two much larger numbers, the radiation from the layer to the ceiling and the re-radiation returned by the ceiling to the layer. Both are decreased, the layer to ceiling because of the lower gas emissivity and the ceiling re-radiation because the ceiling temperature is lower (in response to the decreased heat input from the layer). The net effect turns out to be larger than the net gain just discussed (energy gained from flame radiation minus radiative loss to the floor). Thus the layer actually cools slightly. Note that, if the ceiling had been more thoroughly heat saturated--lower thermal inertia or longer time--the layer temperature would have risen with a decrease in smoke density.

Further numerical experiments showed that, for M05, changing the smoke parameter, FS, from 0.24 to as low as 0.04 had virtually no effect on the upper layer temperature, but reducing the ceiling thermal conductivity (to decrease thermal inertia and reduce the ability of the ceiling to remove heat) and reducing the smoke production raised the gas temperature in agreement with the argument given above.

Although smoke produced had little effect on the thermal predictions, it is obviously important to predicting the smoke measurements. Figure 20 shows the extinction coefficient for mattress M05 computed from doorway smoke measurements [1, figure 54], and computed values for FS = 0.241. Again setting aside the difference in the time to peak, the shape of the curves is quite similar. The comparison suggests that an FS = 0.16 would have been a better choice than the default value, 0.241, for this mattress.

Figure 21 compares the radiation to the non-burning target, object 4, for mattress M05 and a smoke factor FS = 0.24 with the experimental values [1, figure 43]. The trend is generally similar. If, however, the target object is moved relative to the fire, or the fire center moves around on the bed changing its position relative to the target, the contribution of flame radiation will increase as the target and flame approach each other. Figure 22 shows the effect of moving the target to vary target-to-fire spacing. Also indicated on the figure is the bed "diameter". This is the approximate amount the target-to-fire spacing might change as the apparent center of the fire is moved to the extremes of the bed. Note that the dominant contribution to the target heat flux comes from the hot gas layer. This is virtually constant except when the target is very close to the wall. The drop as the wall is approached is due to the changing view factor (the relative amount of the hot layer and cold wall seen by the target). At peak burning the hot gas layer under the ceiling is relatively thick. Its bottom is only about 40 cm above the target. The decrease in heat flux received from the ceiling (as distinct from that received from above due to the hot gas) as the target is moved is also a view factor effect. Because the hot layer is so thick, the target "sees" relatively little of the flame (only that below the layer).

The flame radiation at the target increases as the two approach each other, but is never as large as the hot layer contribution. In these calculations the target was assumed to be a flat, horizontal surface. The Harvard code, level 5, allows the orientation of target surfaces to be varied. Were the target vertical, the heat flux received from the hot gas layer would be somewhat reduced and that coming from the flame would be increased.

## 7. ADDITIONAL MATTRESS SIMULATIONS

The above simulations were for those mattresses where the dominant fuel was flexible urethane foam. As a matter of interest, similar calculations were made for the remaining mattresses in the NBS test series which flamed significantly, M02, 4 and 6. The results are shown in figures 23-25. As in the previous simulations, only input data specific to the particular mattress size, weight of combustible and heat of combustion were used, all other values were the Harvard parameters. The H051 simulation was used with the door narrowed to account for the adjoining structure as already discussed. The results generally compare about as well with experiments as the results obtained with the urethane mattresses. Again, the upper gas temperature is a bit low where the free burn maximum flame height, as computed by, for example, McCaffrey [20], would place the flame tip well above the room ceiling height (M01 and M04). As stated above, this discrepancy is believed to arise either from the failure of current room fire models to account for burning in the hot, upper layer or from inadequacies in the layer radiation computation.

## 8. ROOM "B" SIMULATIONS

As described in [1], two sets of room tests were conducted; one set in the facility shown in figure 12, the second set in a different structure. The burn room for the second set is designated as room "B". The room "B" tests consisted of two series with different ventilation arrangements. Room B was located midway along a corridor which connected at one end to a cross corridor and at the other to a large lobby. In both room "B" test series the room door to the corridor was fully open and the room window closed. In the first series the corridor was force ventilated from the cross corridor end with the ventilation air exiting into the lobby and, from there, to the outside of the building. This series is referred to as the 'ventilated room "B" tests'. The measured flow in the corridor prior to ignition was about  $1.6 \text{ m}^3/\text{sec}$  (compared to a computed flow for the isolated room of  $1.17 \text{ m}^3/\text{s}$  with mattress M05). In the other set no forced ventilation of the corridor and lobby was provided. Doors connecting the fire room, corridor and lobby were open, but all vents to the outside were nominally closed off. The total volume of the room-corridor-lobby complex was  $259 \text{ m}^3$  with a ceiling height of 2.44 m. These are referred to as the 'non-ventilated room "B" tests'. Simulations based on the room "B" geometry were made using the M05 mattress parameters.



In the first set of simulations, the burn room was considered isolated, vented by its door to the atmosphere. As with the room "A" simulations, it was to be expected that the adjoining space would alter the room conditions. The first simulation used the actual door width. The result, for temperature, was quite similar to that shown for room "A" in figure 15. In the room "B" case maximum upper gas temperature was 439 C at 380 sec. The experimental temperatures were much lower, suggestive of a fairly strongly ventilation-limited fire. However, unlike the room "A" simulations, Tanaka's model could not readily be used to estimate the "correct" amount of door closure to use to simulate the remaining structure. The version of his model which was available at the time these simulations were made did not include forced ventilation. Instead, several runs were made with successively smaller door openings. With a 0.2 m door width the peak temperature had increased to 649 C. The fire was oxygen limited from 297 to 455 seconds but the induced flow was large enough to allow a substantial fire. Further closing the door to 0.1 m sufficiently reduced the oxygen available that the peak temperature dropped to 350 C, or nearly to that observed for this mattress in the ventilated room "B" test. The result of the simulations and test are shown in figure 26.

Walter Jones of the Center for Fire Research, in work still in progress, has compared the predictions of single and multi-room models for essentially closed, multi-room configurations quite similar to the non-ventilated series of room "B" mattress burns. Here "single room" means that the volumes of the burn room, corridor and lobby have been combined to define a single, large room with the same ceiling height as the actual room. Jones has found that, for certain purposes, the single room results are better than might, at first, be expected. The single room models do best where doors interior to the multi-room complex are distinctly larger and have shallower transoms than the vents to the outside. Room "B", in the non-ventilated tests would meet these criteria. Accordingly simulations for the non-ventilated series were made for such a single room. Because the predicted temperatures were to be compared to measurements made inside the burn room where the hot gases had had little opportunity to be cooled by contact with the ceiling, the ceiling thermal conductivity was reduced to the assumed conductivity times the artificial (augmented) room area. This would make the convective heat loss to the total ceiling about the same as that lost within the burn room at the same upper gas temperature. The first simulation used a small vent, near the floor. As long as the top of this vent was below the mattress surface its area made little difference. The fire quickly became oxygen limited; the maximum temperature reached was quite low. Next a series of simulations were made with a 2 m high door of increasing widths. (There is no reason to suppose that such leakage as existed came predominantly from floor level.) With a 0.2 m wide x 2 m high door the peak temperature reached 156 C, nearly as high as the test value. Results of these simulations are compared with the test data for a non-ventilated test in figure 27. Although this application clearly stretched the single room model, the simulation suggests that there was substantial leakage in the unventilated case.

Figure 28 shows the calculated height of the lower surface of the hot, upper gas layer for various door openings. Note the slower descent of the layer in the larger (augmented) room than in the actual size (isolated) room. In the actual fire the layer would descend initially as simulated by the isolated room. At around 40 seconds from ignition, when the layer had dropped below the door soffitt (indicated on the right of figure 28), its descent would be retarded as fire gases spilled into the corridor and spread to the lobby. When the layer's descent resumed it would follow more closely the augmented room simulation. Note also that the isolated room with a 0.1 m width door forced the layer down about as far as the 0.2 m door for the augmented room.

The use of a single room for the room "B" tests does not seem justified by the results. They do suggest that the flow situation in the corridor is quite complex with, probably, a great deal of mixing occurring just outside the fire room door. This is consistent with Zukoski's mixing experiments [16] although he has no data on the forced flow "T" configuration encountered here. Note that the flow situation is complicated by the up-wind propagation of the fire gases along the corridor ceiling. The extremely small door openings required to get close to the experimental observations results in a great deal of inter-layer mixing. Because the present model does not include vitiated air burning, the depletion of oxygen in the lower part of the room has no effect on the predicted burning rate. If vitiated burning were included, much less severe flow restriction would almost certainly have been necessary. The basic data and ideas on which to build vitiated air burning models are only just now being developed by CFR supported research. We should be able to address this important, missing, piece of the fire models soon.

## 9. SUMMARY, DISCUSSION AND CONCLUSIONS

Simulations for the seven mattresses considered reproduced the general burn behavior for room A quite well using only three properties specific to the separate mattresses: total weight of combustible, total burn surface area and heat of combustion. The total weight of combustible had a more than six fold variation over the set considered and the simulations showed qualitative differences in behavior from the lightest to the heaviest. Thus combustible weight is clearly an important parameter in assessing mattress burn behavior. Total burn area, for a given weight of combustible, influences both fire intensity and duration. Excluding the control, the lightest and smallest mattress burned to produce the least challenging fire but, had a similar construction been used to make a double bed size mattress, it would have had more combustible and a larger burn area than either of the two mattresses which caused flashover conditions to develop, M01 and M04. It would have been the worst performer rather than the best of the group. That burn area is important is also no surprise. Heats of combustion varied about  $\pm 17$  percent for this sample of seven material assemblies. For this range, the gas temperature could be expected to vary about  $\pm 12$  percent, or about  $\pm 100$  C. This is



a large enough variation that, were it present, one's assessment of the quality of the simulation would suffer. Thus, while not large enough to produce gross changes in behavior, heat of combustion is important to the overall fire assessment.

Smoke production, expressed as grams of particulate per gram of fuel pyrolyzed, did not seem important to thermal behavior for a six fold variation spanning values representative of most materials. Polystyrene would be higher and poly-oxy-methelene lower than the range covered. Smoke production was important for prediction of extinction coefficient and, given suitable input data, the observed behavior could be well represented.

Although some time was spent in studying the rate of heat release data [2, table 5], this test offered little information useful to these simulations;  $\chi$  in [2, table 11] comes from the rate of heat release tests. Note, however, that some test is needed to determine if a mattress will flame. The six mattresses which flamed, and the control, were well modeled by the present fire code. But four mattresses failed to sustain flaming. These would not be well modeled by any of the burn algorithms of the present fire code since they burn in a qualitatively different way from the behavior described by the available simulation algorithms.

It must be remembered that the actual burn behavior of several of the mattresses for which the Harvard model gave reasonable simulations did not burn in the way the model supposes. The model assumes a circular, growing fire on a flat surface. Some of the mattresses melted off substantial amounts of fuel which dripped to the floor and burned under the bed, not on its surface. At the same time, fire was observed on the upper bed surface with the flames of the two merging. M04 was an extreme case of this. This detailed behavior was not simulated, yet the predictions were in fairly good agreement with observations.

It should be kept in mind that some parameters, which were not varied for these simulations, may be very important. For example, heat of pyrolysis and pyrolysis rate are directly related. Heat of pyrolysis was not varied for two reasons: first, because no data was available for the mattresses in question, and, second, because adequate agreement with the experimental burn behavior was obtained by changing the burn algorithm without changing heat of pyrolysis from the nominal value. In some cases, although a parameter is important to burn behavior, its value may actually not vary much in practice. In other cases, most obviously geometry, the parameters are important but we may not know how to assess them. Beds display the fuel in an especially simple geometry. The same material used to build a sofa-bed might burn quite differently in its sofa configuration than in its bed configuration.

To some, the input requirements of the Harvard simulation may seem unreasonably complex. To the fire scientist they all clearly relate to some known, important aspect of fire behavior. It may be that the inputs can be re-cast in a form more readily understood by practicing engineers, but it is doubtful if any can be eliminated. It may be, however, that for broad classes of furnishings, some of the inputs can be left at suitably chosen values and only a much more limited set of variables used to describe the specific behavior of objects from these classes.

During the course of this study a number of changes in the Harvard simulation were studied and several adopted. The simulations were distinctly improved as a result of these changes. There are further improvements, some of them associated with the lower gas layer, which, if made, would further improve the quality of the simulations. Perhaps the most important area for work is related to burning in vitiated air. Improvements are needed both where flames can be expected in the upper layer and where the lower layer is contaminated with combustion products. Studies are underway to provide a sound basis for these changes, but their introduction is probably still a year off. Nearly as important is work related to the pyrolysis rate prediction. The questions of cold fuel radiation absorption and char-formation need to be sufficiently studied and documented so that these clearly important effects can be included in the model.

This study also showed the importance of being able to represent adjacent structure (multi-room model). Although a single room or augmented single room may be able to be adjusted to give good agreement with experiment, the way to adjust it may not be obvious. In this study an appropriate door adjustment for room "A" was deduced from the geometry and confirmed using Tanaka's multi-room simulation. For the room "B" this was not possible and empirical adjustment failed to produce a satisfactory representation of the data. For this case a multi-room simulation was needed.

Finally, much more information is needed on door and window mixing so that the crude correlations used in the new subroutine MIX can be replaced with more general and more accurate forms.

## 10. REFERENCES

- [1] Babrauskas, V., "Combustion of Mattresses Exposed to Flaming Ignition Sources, Part I. Full-Scale Tests and Hazard Analysis", Nat. Bur. of Stand. (U.S.) NBSIR 77-1290 (1977).
- [2] Babrauskas, V., "Combustion of Mattresses Exposed to Flaming Ignition Sources, Part II. Bench-Scale Tests and Recommended Standard Test", Nat. Bur. of Stand. (U.S.), NBSIR 80-2186 (1980).
- [3] Emmons, H.W., "Computer Fire Code II", Home Fire Project Technical Report No. 20, Harvard University, Cambridge, MA, 1977.

- [4] Emmons, H.W., Mitler, H.E., Treffethen, L.N., "Computer Fire Code III", Home Fire Project Technical Report No. 25, Harvard University, Cambridge, MA, 1978.
- [5] Mitler, H.E., "The Physical Basis for the Harvard Computer Fire Code", Home Fire Project Technical Report No. 34, Harvard University, Cambridge, MA, 1978.
- [6] Mitler, H.E., Emmons, H.W., "Computer Fire Code V", Home Fire Project Technical Report No. 45, Harvard University, Cambridge, MA, 1981.
- [7] Croce, P.A., Emmons, H.W., "The Large-Scale Bedroom Fire Test, July 11, 1973", FMRC Serial No. 21011.4, Technical Report R.C. 74-T-31, Factory Mutual Research Corp., Norwood, MA, July 1974.
- [8] Croce, P.A., "A Study of Room Fire Development: The Second Full-Scale Bedroom Test of the Home Fire Project (July 24, 1974), Volumes I and II", FMRC Serial No. 21011.4, Technical Report, RC75-T-31, Factory Mutual Research Corp., Norwood, MA, June 1975.
- [9] Alpert, R.L., Modak, A.T., Newman, J.S., "The Third Full-Scale Bedroom Fire Test of the Home Fire Project (July 30, 1975)", FMRC Serial No. 21011.6, Factory Mutual Research Corp., Norwood, MA, Oct. 1975.
- [10] Babrauskas, V., "Will the Second Item Ignite?", Nat. Bur. of Stand. (U.S.) NBSIR 81-2271 (1981).
- [11] Babrauskas, V., private communication.
- [12] Kashiwagi, T., "Radiative Ignition Mechanism of Solid Fuels", Fire Safety Journal, Vol. 3, 185-200 (1981).
- [13] Orloff, L., "Simplified Radiation Modeling of Pool Fires", Factory Mutual Research Corp., Norwood, MA 02062, Jan. 1980 (Paper for presentation at the 18th Symposium (Intl.) on Combustion, University of Waterloo, Ontario, Canada, Aug. 1980).
- [14] McCaffrey, B.J. and Rockett, J.A., "Static Pressure Measurements of Enclosure Fires", Journal of Research, Nat. Bur. of Stand., Vol. 82, No. 2, Sept.-Oct. 1977.
- [15] Quintiere, J.G. and McCaffrey, B.J., "The Burning of Wood and Plastic Cribs in an Enclosure", Vol. 1, Nat. Bur. of Stand. (U.S.) NBSIR 80-2054 (1980).
- [16] Zukoski, E.E., "Progress Report for Nov. 20, 1980, Experimental Study of Environment and Heat Transfer in a Room Fire", Cal. Inst. of Tech., Pasadena, CA, Nov. 20, 1980.

- [17] Tu, King-Mon, "The Calibration of a Burn Room for Fire Tests on Furnishings", NBS Technical Note 981, U.S. Department of Commerce, Washington, DC, Dec. 1978.
  
- [18] Tanaka, Takeyoshi, "A Model on Fire Spread in Small Scale Buildings, 2nd Report", Building Research Institute, Ministry of Construction, Tokyo, Japan, March 1980.
  
- [19] Tewarson, A., "Physico-Chemical and Combustion/Pyrolysis Properties of Polymeric Materials", Nat. Bur. of Stand. (U.S.) NBS-GCR-80-295 (1980).
  
- [20] McCaffrey, B.J., "Purely Buoyant Diffusion Flames: Some Experimental Results", Nat. Bur. of Stand. (U.S.) NBSIR 79-1910 (1979).



APPENDIX I. THE EFFECT OF A THIN CHAR LAYER ON PYROLYSIS RATE

The argument is as follows: We start with the heat flux reaching the fuel surface as calculated for a flame with the final, desired pyrolysis rate. We also determine the heat needed to pyrolyze fuel at the desired rate, 46 g/sec. The difference between these two must be lost by the surface. This can happen by three mechanisms -- surface radiation, convection and conduction into the fuel body. We ignore convection and neglect the conduction loss here; all the heat is to be carried away by radiation. Now, using the thermal properties of charcoal given in [A1.1], the heat conducted through a char layer can be found as a function of the layer's thickness and the temperature difference across the layer. We know the temperature at the fuel-char interface must be the pyrolysis temperature and that the heat which must be transmitted is the amount needed to pyrolyze the fuel. As stated above, we also know the amount that must be radiated from the char surface. These conditions are used to find the char surface temperature and thickness.

Radiation reaches the fuel from three sources: the flames over the surface itself, the hot gas layer trapped under the ceiling and the ceiling (attenuated by absorption in the hot layer). These are reported outputs of the Harvard simulation. Their sum, for a mattress fire burning at 46 g/sec., is 96.8 kW/m<sup>2</sup>.

The fire area at this point was 2.446 m<sup>2</sup>, giving a pyrolysis rate of 18.8 g/sec-m<sup>2</sup>. Taking the Harvard default heat of pyrolysis, 2.05 MJ/kg, the heat needed at the fuel surface is 18.8 x 2.05 = 38.5 kW/m<sup>2</sup>.

Therefore the heat that must be lost from the surface by radiation is

$$96.8 - 38.5 = 58.3 \text{ kW/m}^2$$

Assuming a black surface with unit emissivity, the surface temperature must be

$$\sigma T^4 = 5.67 \times 10^{-11} \times T^4 = 58.3 \text{ kW/m}^2$$

or

$$T = 1007^\circ\text{K}$$

Taking the Harvard default pyrolysis temperature, 600°K, the char thickness which will transmit 38.5 kW/m<sup>2</sup> with a temperature difference of

$$1007 - 600 = 407^\circ\text{K}$$

is

$$38.5 = (k/d) \times 407$$

$$(k/d) = 0.0947 \text{ kW/m} - ^\circ\text{K}$$

[17, p. 1784] gives  $k = 0.37 \text{ BTU/hr-ft-F/in}$  for char, or

$$k = 5.33 \times 10^{-5} \text{ kW/m} - ^\circ\text{K}$$

Therefore

$$d = 0.56 \text{ mm}$$

#### References

- [A1.1] Hodgman, C.D., "Handbook of Chemistry and Physics", Twenty-Seventh Edition, Chemical Rubber Publishing Co., Cleveland, Ohio, 1943.

## APPENDIX II. HOT-COLD GAS MIXING AT VENTS

Inclusion of mixing at the vents entails a number of changes throughout the program as the implications of the changed properties of the lower gas layer in the room are accommodated. To date only a fraction of all the "consistent" changes have been made and only those made will be discussed. The changes described here were made in a way to least disrupt the H05 code. It is intended that they should be fully integrated in the code structure, but only after their general operation has been debugged.

Because the mixing information is needed in a number of subroutines, a new COMMON, CVENT3 was added. It provides communication throughout the program.

One effect of mixing is to vitiate the air in the lower gas layer. This results in a change in the stoichiometric coefficients, XGAMMA and XGAMAS, which are defined in terms of amount of air rather than amount of oxygen needed to fully burn the pyrolysis products of each object. This is done by storing initial values in CVENT3 and adjusting XGAMMA and XGAMAS by the ratio of ambient to actual lower layer oxygen mass fraction as vitiation occurs. Initial values for the stoichiometric coefficients are obtained in INPUT3 and initialized in CVENT3 in LAYR. The initial values are called STOIC1 and STOIC2. During each iteration XGAMMA and XGAMAS are adjusted using

$$\begin{aligned} \text{XGAMMA} &= \text{STOIC1} \times 0.2318/\text{ZYCO} \\ \text{XGAMAS} &= \text{STOIC2} \times 0.2318/\text{ZYCO} \end{aligned}$$

where ZYCO is the oxygen mass fraction in the lower gas layer.

Another effect of the vitiation of the lower layer is to reduce the smoke production. Data on this effect is still scarce [A2.1] so the correlations used only express the trend. The input smoke production constant is FS. It is set for each object in INIT, carried in CVENT3 as FSINIT and corrected in LAYR according to

$$\text{FS} = \text{FSINIT} \times \text{ZYCO} / (0.2318 + 2 \times \text{FSINIT} \times (\text{ZYCO} - 0.2318))$$

ZUFZZ is the extinction coefficient for the flame brush. It is adjusted using a similar functional relation; the initial value, stored in CVENT3 is ZUFI.

H05 makes no provision for entering emissivities for the floor, walls or ceiling of the room. In H051 default values of 0.82 are set in LAYR and carried in CVENT3 as ECEIL and EFLOOR. The upper walls are assumed to have the same characteristics as the ceiling and the lower walls those of the floor. No provision has yet been made to input alternative values.

Within the subroutine MIX two operations are performed: first, following the definition of Zukoski [16], a Richardson number is found. Next, this is used in an empirical data correlation to find the amount of mixing flow leaving the hot layer. Several data correlations for the amount of mixing were tried. A slight modification of the one used by Quintiere [15] was adopted. He calculates the mixing flow using

$$\frac{\dot{m}_m}{\dot{m}_i} = \left( \frac{W}{W_c} \right)^{1/4} K \left( \frac{\rho_L}{\rho_o} \right) (1 - D/N)$$

where

- $\dot{m}_m$  = mass flow transferred from the hot layer to the cool layer
- $\dot{m}_i$  = mass flow entering the door
- $W^i$  = width of the wall containing the door
- $W$  = width of door
- $K^c$  = constant set equal to 1/2, c.f. [15]
- $\rho_L$  = density of the hot layer
- $\rho_o$  = density of the entering gas
- $D^o$  = height of the hot-cool interface in the room
- $N$  = height of the neutral plain in the doorway
- $n$  = 1/4

Note that, in this form, the door width correction  $(W/W_c)$  increases indefinitely as this ratio increases. Actually one suspects<sup>c</sup> (there is little good data) that, beyond a certain point, increasing the space around a door will no longer increase the amount of mixing. To retain the dependence expressed by Quintiere's expression for values of the ratio near unity, yet have it approach a constant for large values, the expression

$$[1 + 3(W/W_c)] / [2(1 + W/W_c)]$$

was used. The asymptotic value, 3/2, was chosen somewhat arbitrarily.

To use Quintiere's mixing correlation a value for  $(1 - D/N)$  is needed. This is obtained, again following Quintiere, from the basic door flow equation (slightly simplified)

$$\frac{\dot{m}_i}{W_c} = \frac{2}{3} C \rho_o \sqrt{2g \frac{(\rho_L - \rho_o)}{\rho_o}} \quad [\sqrt{N - D} (N + D/2)]$$

where

$$C = \text{orifice flow coefficient} = 0.68$$



This relation cannot be readily used with the present VENT subroutine of the Harvard code as the neutral plain height, N, is not directly available. It can be expressed in terms of Zukoski's Richardson number

$$Ri = g(\rho_L - \rho_o) D/u_i^2$$

but, since

$$u_i = \dot{m}_i / \rho_o W_c D$$

$$Ri = g\rho_o(\rho_L - \rho_o) D^3 (W_c / \dot{m}_i)^2$$

This leads to a cubic equation for  $(1 - N/D) = x$  whose solution it is desirable to side-step.

or

$$Ri = \frac{9}{8C} \left(\frac{D}{N}\right)^3 / [(1 - D/N)(1 + D/2N)]$$

$$x(3 - x)^2 = 4R(1 - x)^3$$

$$R = 9/(8C Ri)$$

This is done by noting that a very good approximation to the solution is

$$x = 4R / [(9 + 12R) - x_1(6 + 12R) + x_1^2(1 + 4R)]$$

$$x_1 = 4R / (9 + 4R)$$

It must be stressed that this correlation is based on data for doors. Windows are known to produce much more vigorous mixing, especially when the hot-cool interface in the room is below the window sill [16].

The hot, and now also the cool layer characteristics are calculated in subroutine LAYR. The procedure used for the hot layer is augmented with parallel calculations for the cool layer. For each vent the mixing flow and rate of transport from the hot layer of energy, oxygen, CO<sub>2</sub>, CO, H<sub>2</sub>O and particulate/aerosol are summed. These rates are combined with corresponding ambient quantities entering through the lower part of the vents. Loss rates from the lower, cool layer for the same quantities are determined from the gas entrained by all the fire plumes. The accretion less loss, for each of these quantities, is integrated to give the current amount of each in the cool layer. Mass fractions are also computed.

The mass fraction of oxygen in the cool layer is then used to correct XGAMMA, XGAMAS, FS and ZUFZZ as discussed above.

Because the cool, lower layer is contaminated by smoke and combustion products, it can absorb radiation and re-radiate to its surroundings. The cool layer emissivity/absorptivity is calculated by a method similar

to that used in RDNL for the hot, upper layer. The calling statements for ABSRB2 and ABSRB3 have been changed to facilitate this. The cool layer energy balance currently includes radiant energy incident from the ceiling and hot layer above it and from the cool walls and floor which surround its remaining sides\*. Lower vent areas are treated as radiating at the same temperature as the walls. Radiant energy from flames is also included. The cool layer radiates to all its surroundings.

The radiation balance used is similar to but slightly more inclusive than that used by H05 and RDNL for the hot, upper layer. The correct calculation of radiative equilibrium between two non-planar surfaces at different temperatures separated by two absorbing and radiating gas layers with different emissivities and temperatures is a rather complicated problem [A2.2]. Adding a conical flame volume would still further complicate the already difficult situation. The equations currently programmed in H051 are outlined in figure A2.1. They approximate the actual room by a pair of parallel planes separated by two emitting/absorbing gas layers with differing characteristics. Gas emissivities are based on a mean beam length =  $4kV/A$ . Two pairs of radiant flux equations are written for the upward and downward streaming fluxes in each layer. Four matching conditions are set up at the upper and lower boundaries of the layers. The flux equations are solved in a new subroutine, FLUX, called from RDNL. The quantities returned are the net radiant energy lost by the upper, hot gas layer to the ceiling,  $FL1 = e_w (I_1 - T_w^4)$ , the net radiant energy lost by the upper layer to the lower, cool gas layer,  $FL2 = (I_2 - I_3)$ , and the net radiant energy lost by the lower layer to the floor,  $FL3 = e_f (I_4 - T_f^4)$ .

The flame radiation contribution to the lower layer is computed in RDNL. There the flame radiation to the upper layer is found assuming the radiation comes from a point source one flame radius above the fuel surface. The radiation incident on the lower layer, TEPCR, is the total flame radiation less that incident on the hot layer and less that which intercepts the fuel surface.

$$TEPCR = e_c \sum_{\text{plumes}} TEPR \times 1/2 [(1 + \cos(\theta)) - (1 - \cos(\theta_1))]$$

where

TEPR = total flame radiation

$$\cos(\theta) = h / \sqrt{h^2 + r_L^2}$$

$$\cos(\theta_1) = r_s / \sqrt{r_s^2 + r_s^2}$$

$r_L$  = WL/ = "radius" of the upper layer

$r_f$  = radius of the fire

$r_s$  = radius of the fuel surface

$e_c$  = lower layer emissivity

\*Note that the present Harvard code does not allow the lower walls to be heated, they remain at the "outdoor" ambient.

The upper layer radiant energy gain is

$$- \sigma(A_H - WL - Avt) FL1 - \sigma WL FL2 - \sigma Avt (T_H^4 - T_A^4) \\ + \text{flame contribution as calculated in H05.}$$

The lower layer radiant energy gain is

$$TECZR = \sigma WL FL2 - \sigma(A_C - WL) FL3 + TEPCR$$

TECZR is passed to LAYR via CVENT3.

The calculations reported in this paper were done with an intermediate version of the mixing calculation which did not include flame radiation absorbed by the cool layer. It also used the upper layer radiation absorption as given in the Harvard simulation, level V - i.e., the upper layer saw the lower layer and floor at the now elevated room ambient temperature.

For M01, using the upper layer radiation balance as detailed in this appendix, raised the peak temperature about 55°C. Including flame radiation in the lower layer radiative balance raised the peak temperature, for M01, an additional 65°C. Adjusting the stoichiometric coefficients had no appreciable effect. With all these changes, as described here, for M01, the peak temperature was 886°C at 420 sec compared to 768°C calculated at 420 sec as shown in figures 13 and 14. Lower layer temperature was 265°C compared to 378°C as shown in figure 14. The hot-cool interface had moved down 0.1 m to 1.0 m. With this improved treatment of radiation, overall, the simulation was significantly closer to the test data for M01 and M04, and slightly closer for M02, 5, 6 and 9. The room B simulations were about the same but, as noted in the main text, the single room model really couldn't deal adequately with this complex geometry.

#### References

- [A2.1] Santo, G., "Influence of Oxygen Depletion on the Radiative Properties of PMMA Flames", Factory Mutual Research Corp., FMRC J.I. OAOE6.BU-3, RC79-BT-6, Norwood, Mass., August, 1979.
- [A2.2] Siegel, R. and Howell, J.R., "Thermal Radiation Heat Transfer", NASA SP-164, National Aeronautics and Space Administration, Washington, D.C., 1971.

### APPENDIX III. DOOR FLOWS

Dr. Tanaka's model, unmodified, yielded a single room flow at the time of peak burning of 0.49 Kg/sec; the Harvard code 1.10 Kg/sec. To choose between the two, the data of Steckler [A3.1] was referred to. The Harvard code prediction of the flow in Steckler's room, which discharged into a not too large plenum but one equipped with an exhaust vent directly over the door, is compared with the measured values in figures A1 and A2. The prediction is about 10 percent low. The Harvard code makes no provision for interaction of the fire plume and door jet as discussed in [A3.2], so it is not surprising that the prediction is low. The amount of plume-door jet interaction to include is obviously a function of the room and object geometry. Furnishings may not be placed as favorably for a strong interaction as in Steckler's fire and objects between the door and principal fire may break up the door jet. On the whole, the Harvard code predictions seem quite satisfactory, and, by inference, Tanaka's seem too low for the type of burner used by Steckler. After modification, the Tanaka code gave a flow of 1.2 kg/sec., slightly higher than H051 and very close to the Steckler data.

#### References

- [A3.1] Steckler, K.D., "Fire Induced Flows Through Room Openings - Flow Coefficients", Nat. Bur. of Stand. (U.S.), to be published.
- [A3.2] Quintiere, J.G., Rinkinen, W.J., and Jones, W.W., "The Effect of Room Openings on Fire Plume Entrainment", Combustion Science and Technology (to be published).



Table 1. The computed effect of adjacent, connected rooms on the fire induced flow from room "A"

<u>Item</u>	<u>Room 1 of 1</u>		<u>Room 1 of 3</u>	
Q	1.0	MW	1.0	MW
time	366	sec	366	sec
T layer	702	K	742	K
vent out-flow	1.20	kg/s	0.90	kg/s
vent in-flow	1.20	kg/s	0.90	kg/s
layer depth	1.60	m	1.66	m
Q	0.125	MW	0.125	MW
time	372	sec	372	sec
T layer	387	K	399	K
vent out-flow	0.86	kg/s	0.66	kg/s
vent in-flow	0.86	kg/s	0.65	kg/s
layer depth	1.51	m	1.59	m

Ratios

$$\begin{aligned} \text{Flow (1 of 3)/flow (1 or 1)} &= 0.899/1.200 = 0.749 \\ &0.660/0.862 = 0.766 \\ &0.653/0.859 = 0.760 \end{aligned}$$

$$\begin{aligned} \text{H051 (70.7\% door)/(100\% door)} &= 0.854/1.105 = 0.773 \\ \text{(50.0\% door)/(100\% door)} &= 0.653/1.105 = 0.591 \end{aligned}$$

Table 2. The effect of a change of the smoke parameter, FS

Mattress M01

<u>Item</u>	<u>Run 191</u>		<u>Run 192</u>	
FS	0.241		0.120	
time	420	sec	420	sec
Q	1.84	MW	1.84	MW
T upper	1041	K	1021	K
T ceiling	984	K	953	K
T lower	651	K	614	K
T ambient	293	K	293	K
Smoke fraction	0.0274		0.0141	
Extinction Coefficient	7.25/m		3.74/m	
Emissivity *	0.978		0.946	
Layer Energy Balance				
Stored	-2	kW	-6	kW
Plume convection	1797	kW	1764	kW
Door convection	-902	kW	-898	kW
Net convection	895	kW	866	kW
Inter-layer mixing	-162	kW	-150	kW
Ceiling convective heating	-83	kW	-100	kW
Radiation, hot layer to:				
Ceiling (net)	-328	kW	-351	kW
Out vents	-41	kW	-37	kW
Lower layer	-770	kW	-689	kW
Flames	487	kW	456	kW
Net gain	-652	kW	-621	kW

\*  $e = 1 - \text{EXP}(-z/(1 + 0.18z))$

$z = 4 \text{ kV/A}$

V = layer volume

A = layer surface area

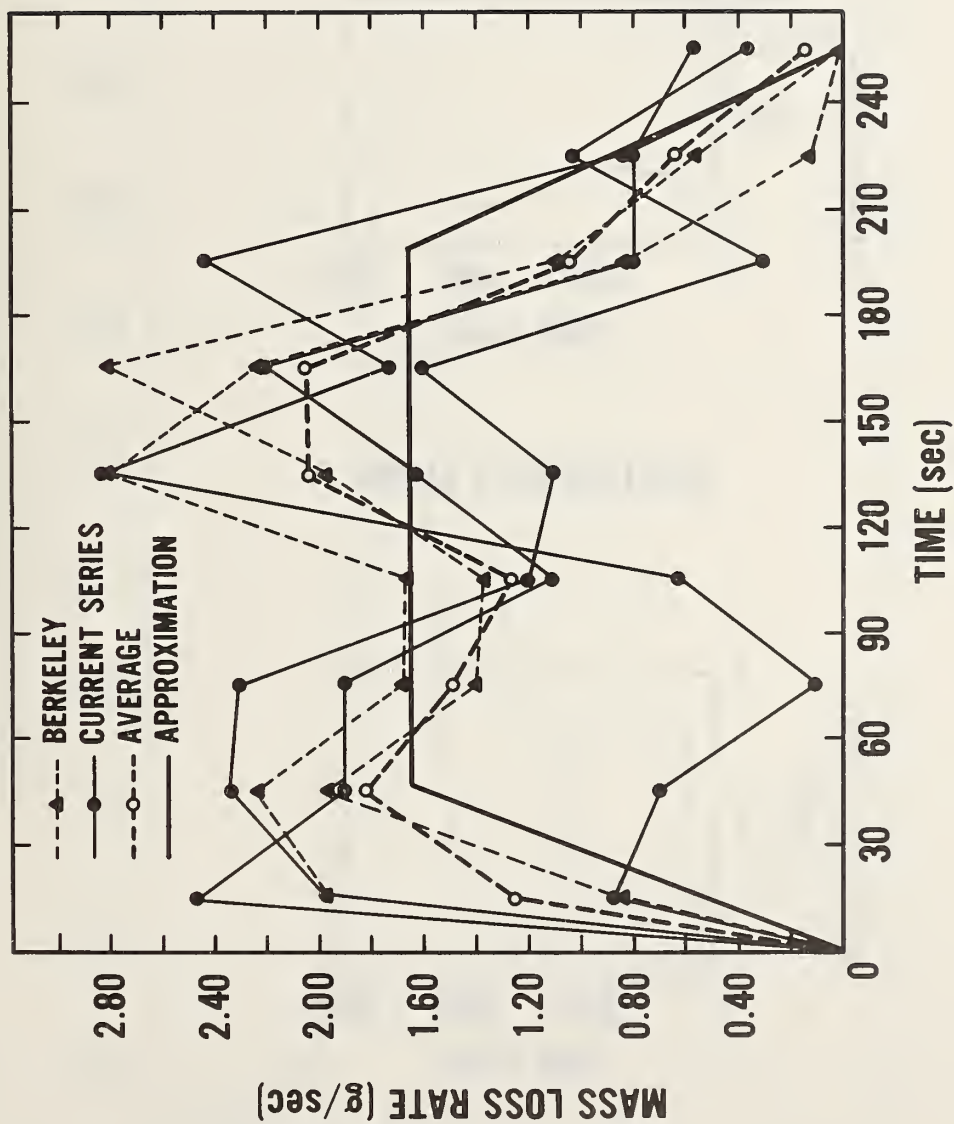
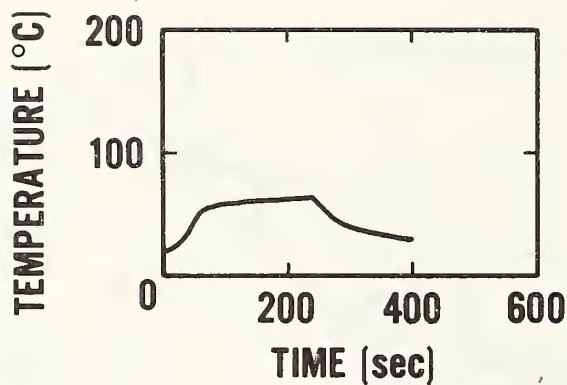


Figure 1. Burning rate versus time for 5 standardized wastebaskets. Also shown are the average burning rate versus time and the burning rate to be simulated.

Figure 2a. Calculated temperature versus time for the standardized wastebasket burned alone. Temperature and time scales are the same as will be used for mattress data.



### WASTEBASKET ALONE

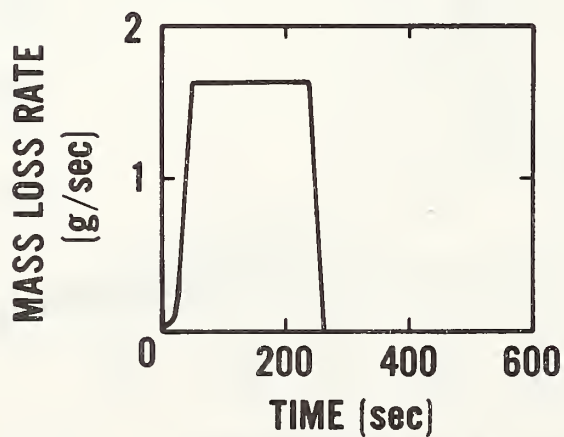


Figure 2b. Mass loss rate versus time for wastebasket simulation. Vertical scale 12 X that used for mattress data.



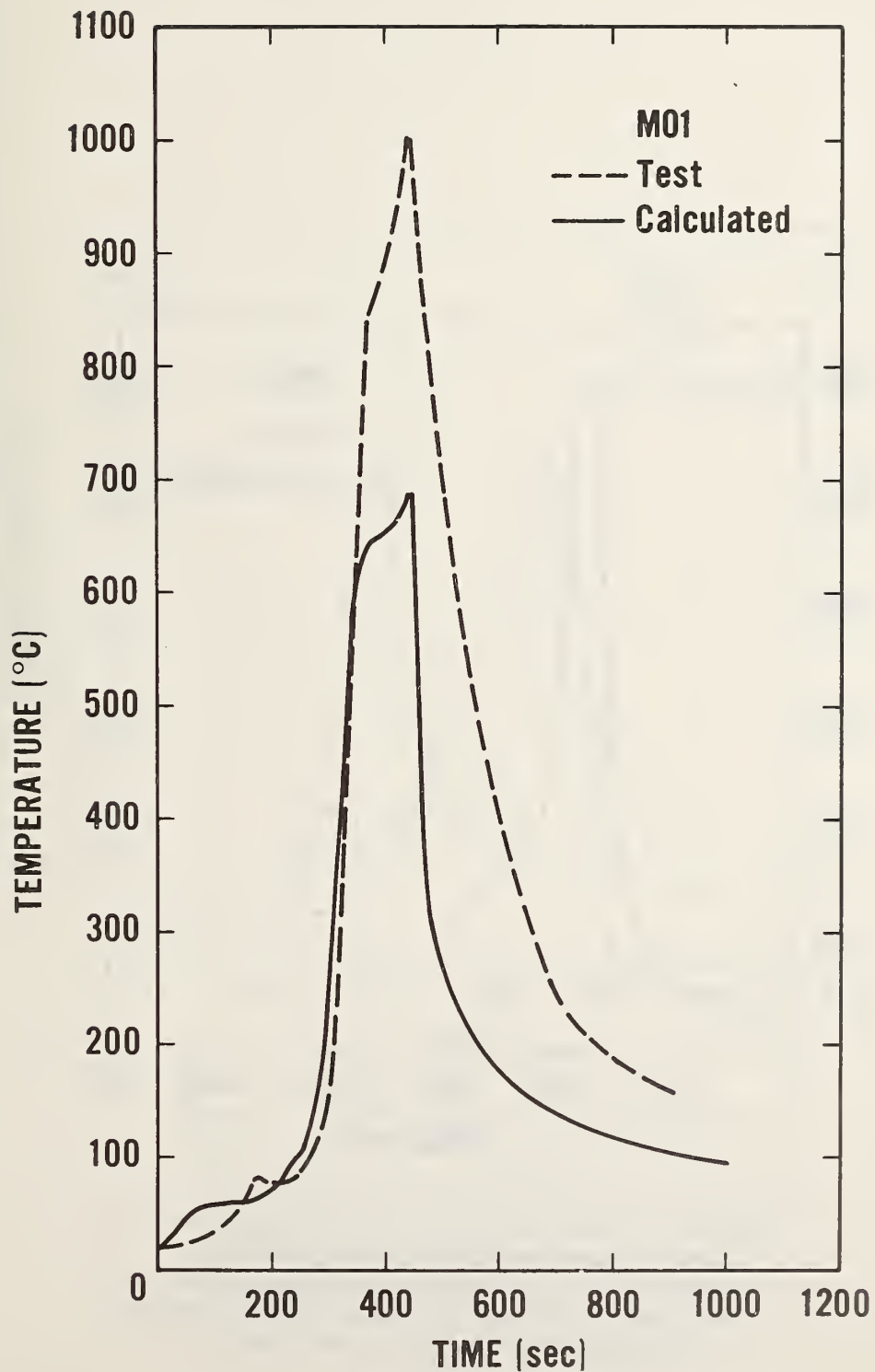


Figure 3. Room upper gas temperature versus time for mattress M01 (data from [1, figure 17]). Also shown is the calculated hot layer temperature using Harvard default values except as noted in the text.

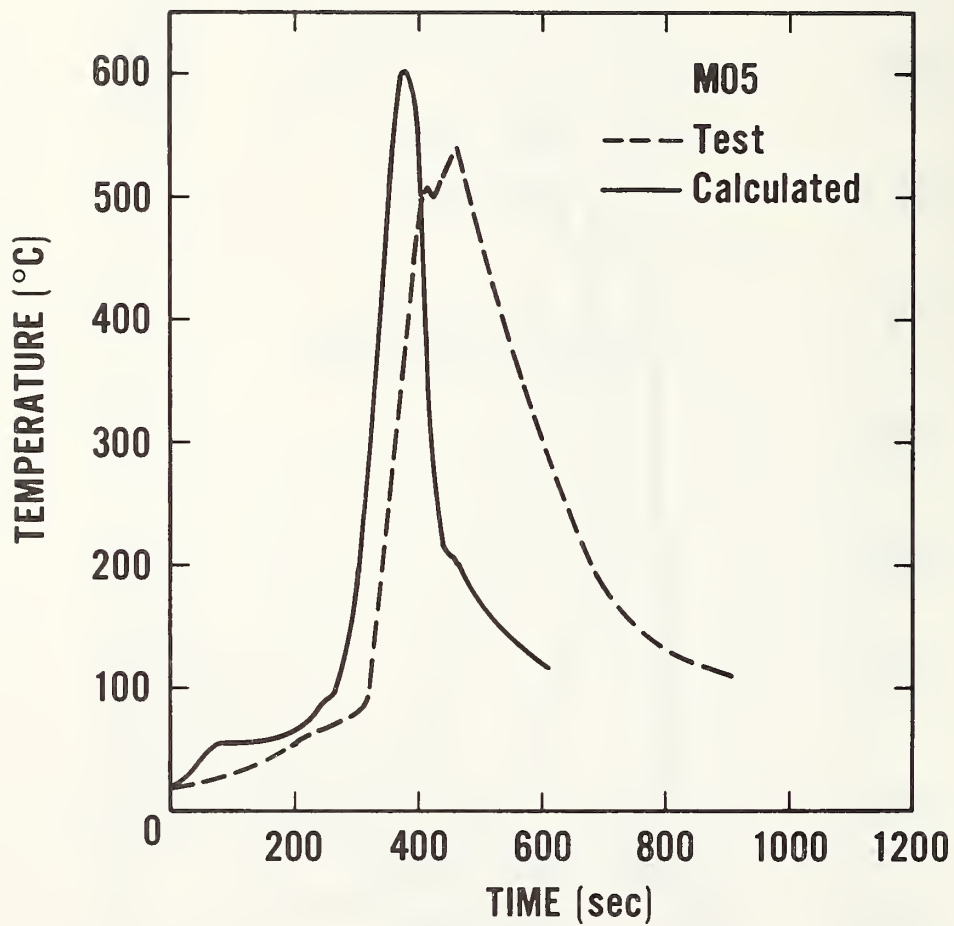


Figure 4. Room upper gas temperature versus time for mattress M05 (data from [1, figure 21]). Also shown is the calculated hot layer temperature using Harvard default values except as noted in the text.

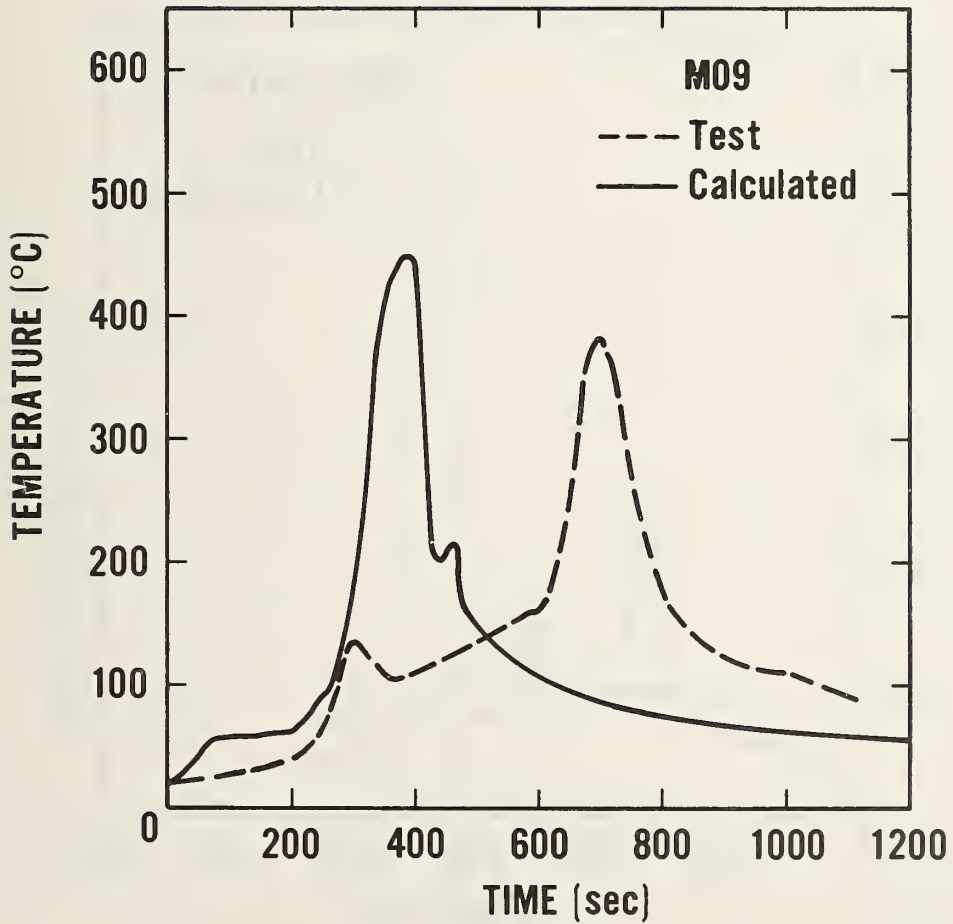


Figure 5. Room upper gas temperature versus time for mattress M09 (data from [1, figure 25]). Also shown is the calculated hot layer temperature using Harvard default values except as noted in the text. The small hump at 450 seconds on the calculated temperature curve is caused by ignition and burning of the pillow. At this point the mattress burned, has terminated.

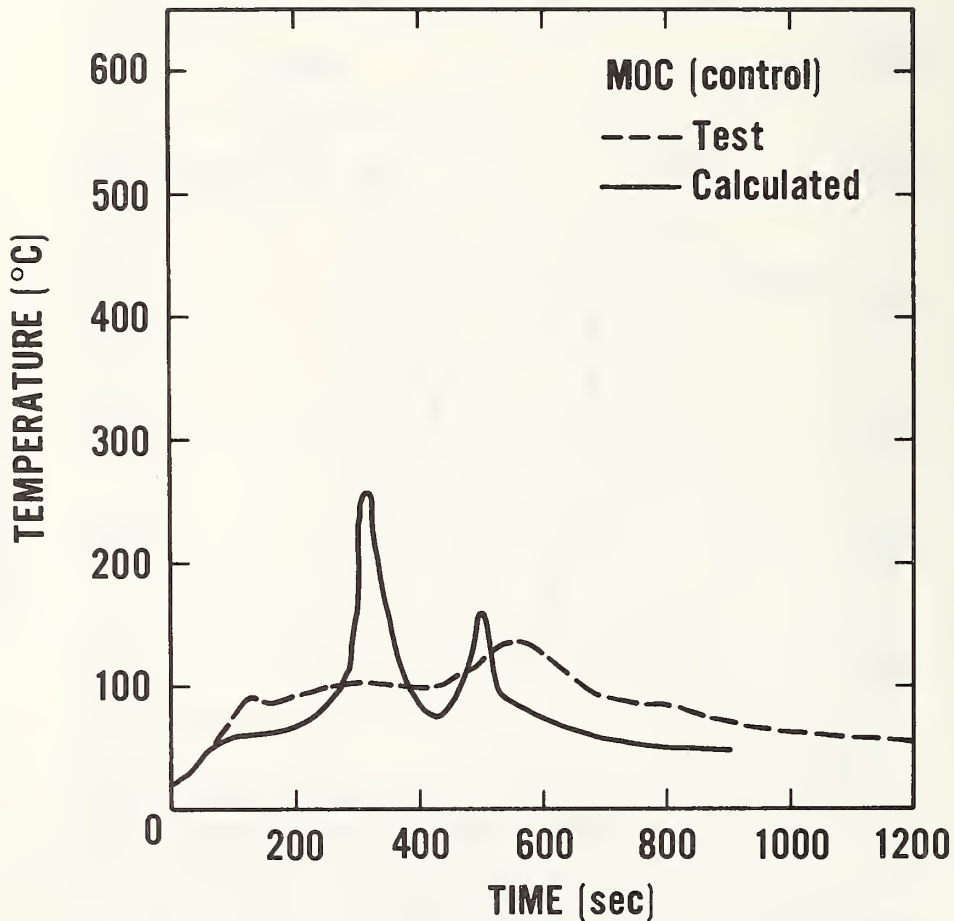


Figure 6. Room upper gas temperature versus time for control mattress (data from [1, figure 16]). Also shown is the calculated hot layer temperature default values except as noted in the text. The small hump at 500 seconds on the calculated temperature curve is caused by the pillow burning. At this point the bedding is burned out. This peak occurs slightly later than for the other mattresses due to the slower rate of growth of this relatively small fire.



Figure 7. Mass loss rate as a function of time for mattress M05 (data from [1, figure 13]). Also shown is the calculated mass loss rate using the Harvard default values except as noted in the text.

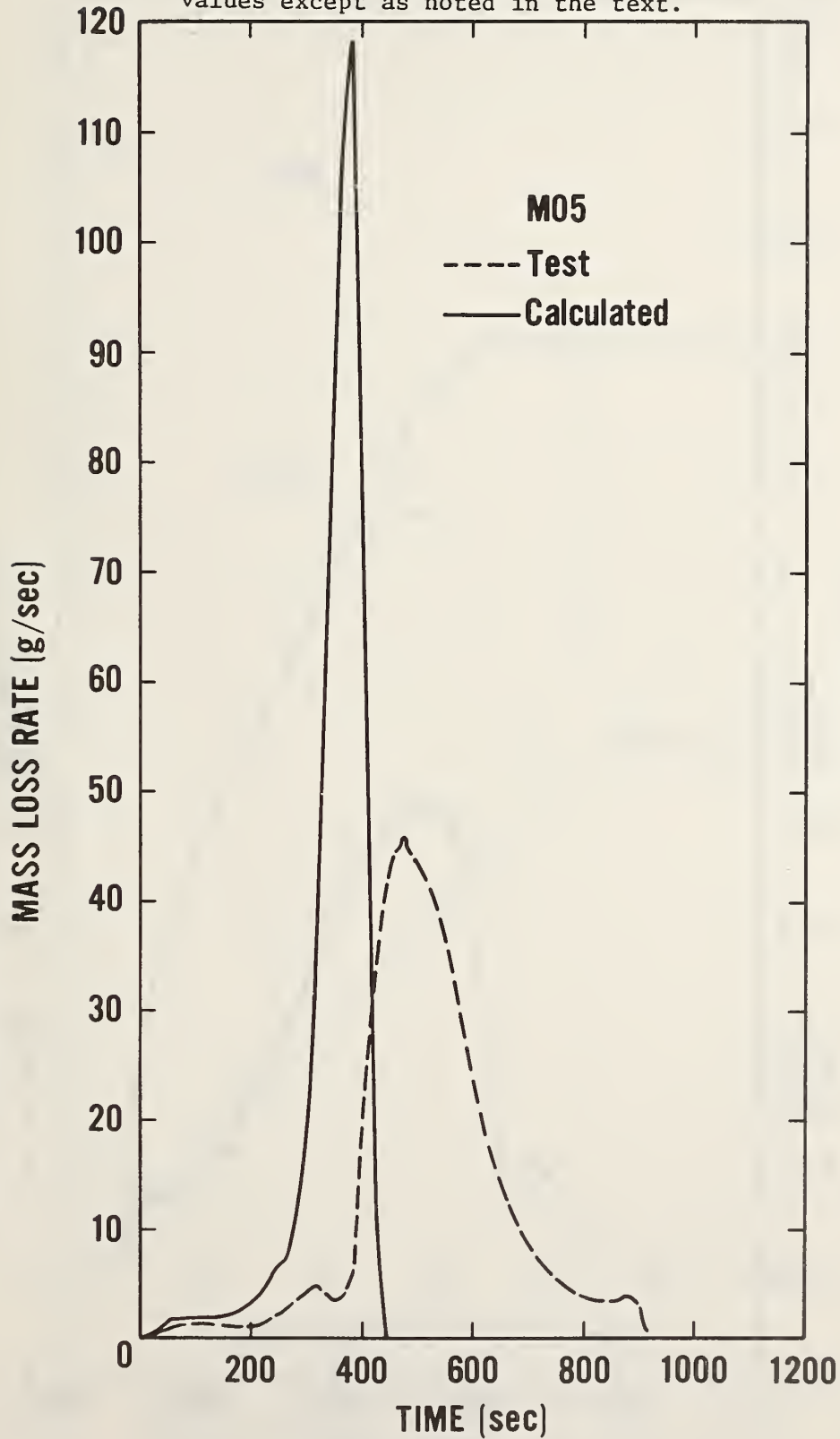
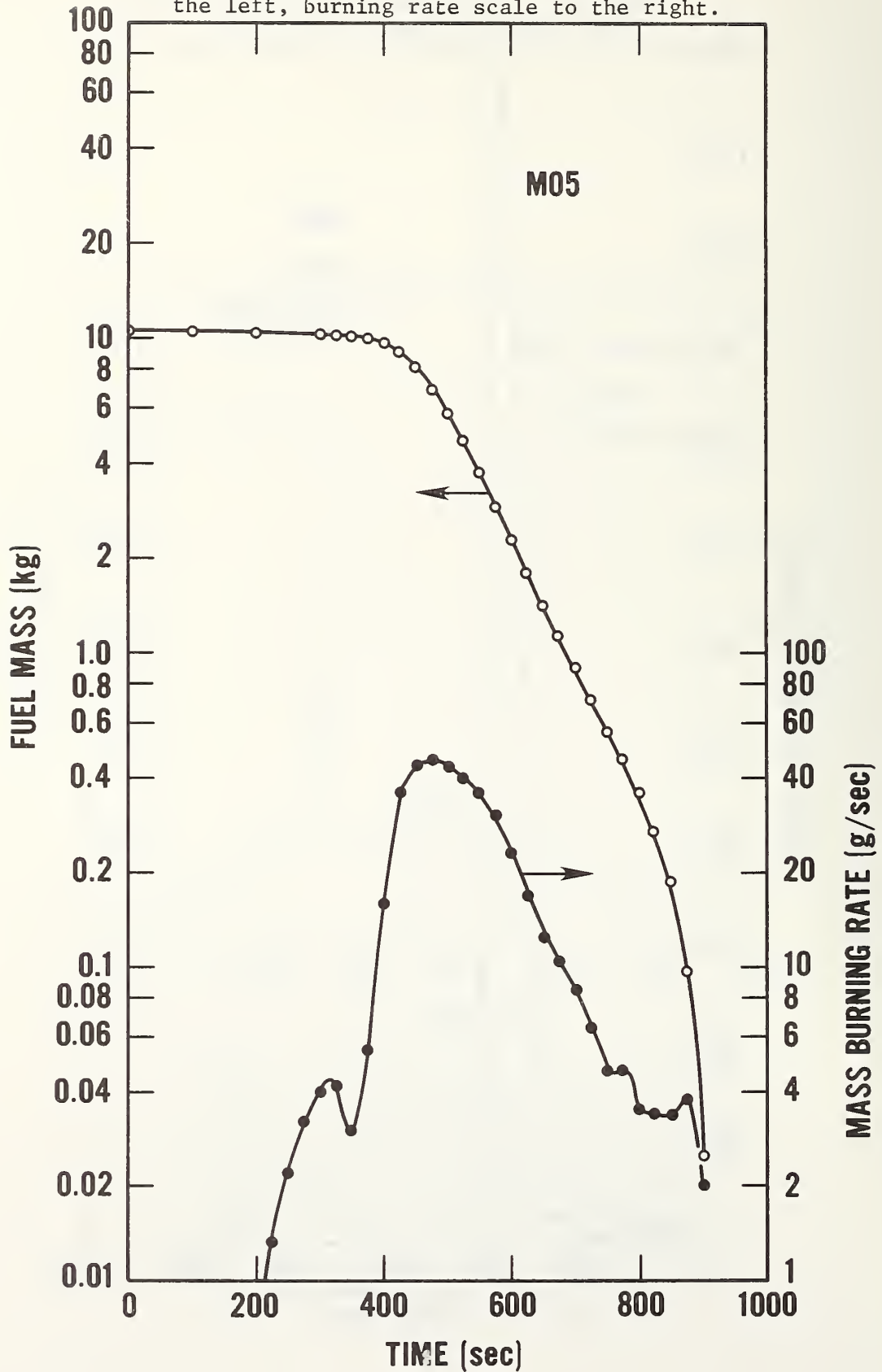


Figure 8. Semi-log plot of experimentally determined fuel mass and mass burning rate for mattress M05 (data from [1, figure 13]) and numerical integration). Mass scale to the left, burning rate scale to the right.



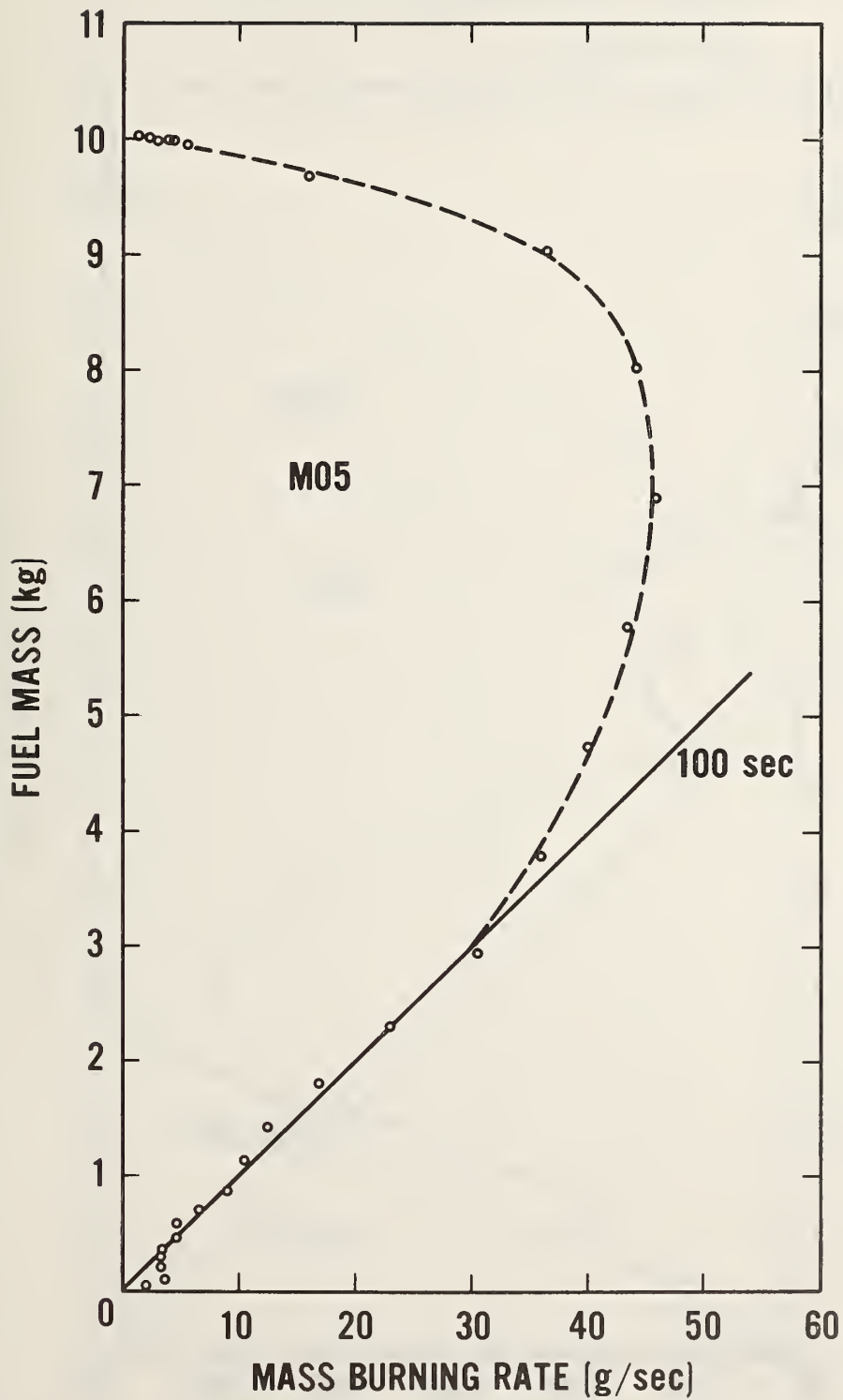


Figure 9. Remaining fuel mass plotted against mass burning rate for mattress M05. Straight line corresponds to a "late burning constant" of 100 seconds (10 g/sec/kg fuel remaining).

Figure 10. Remaining fuel mass plotted against mass burning rate for mattress M09. Straight line corresponds to a "late burning constant" of 100 seconds (10 g/sec/kg fuel remaining).

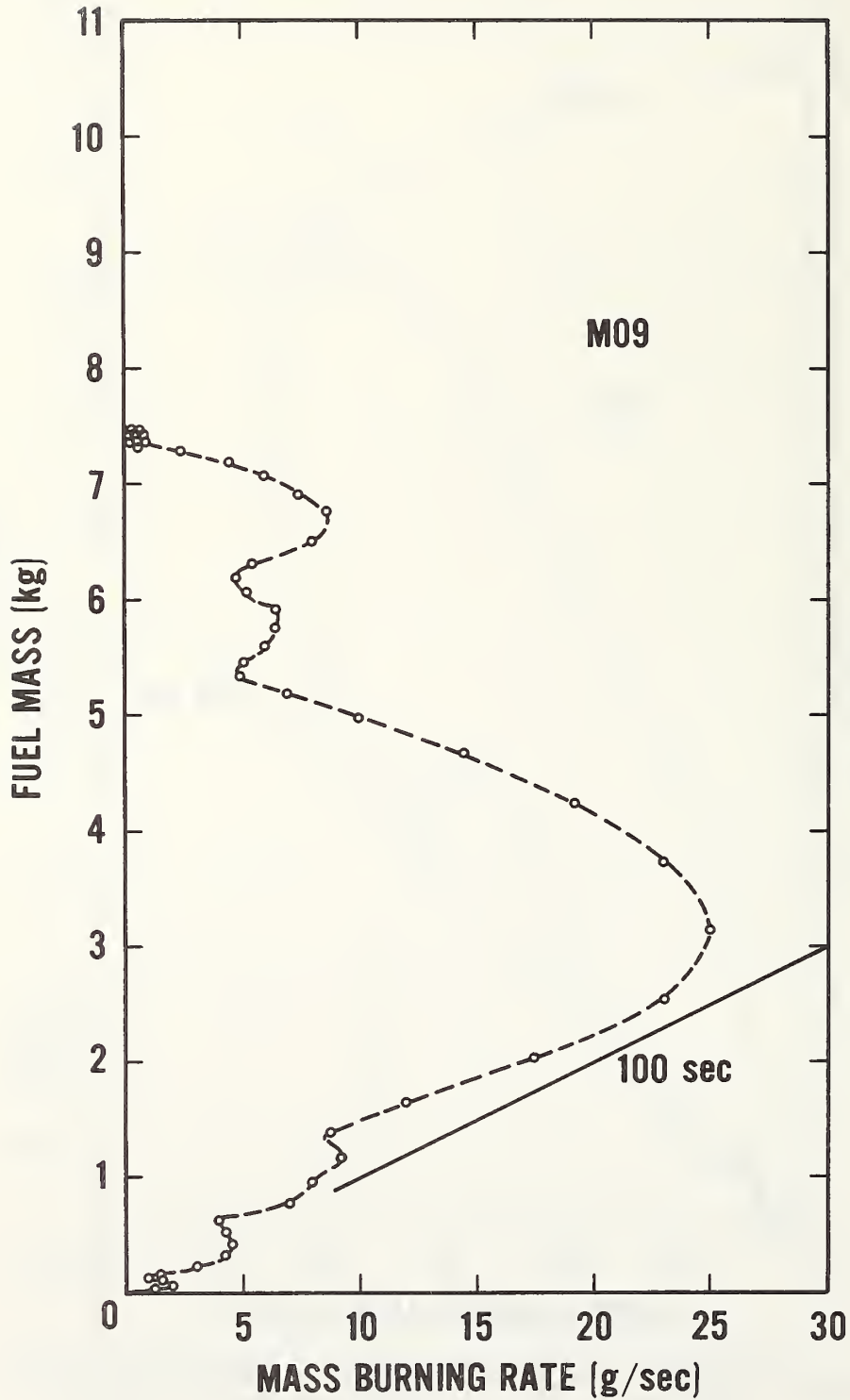
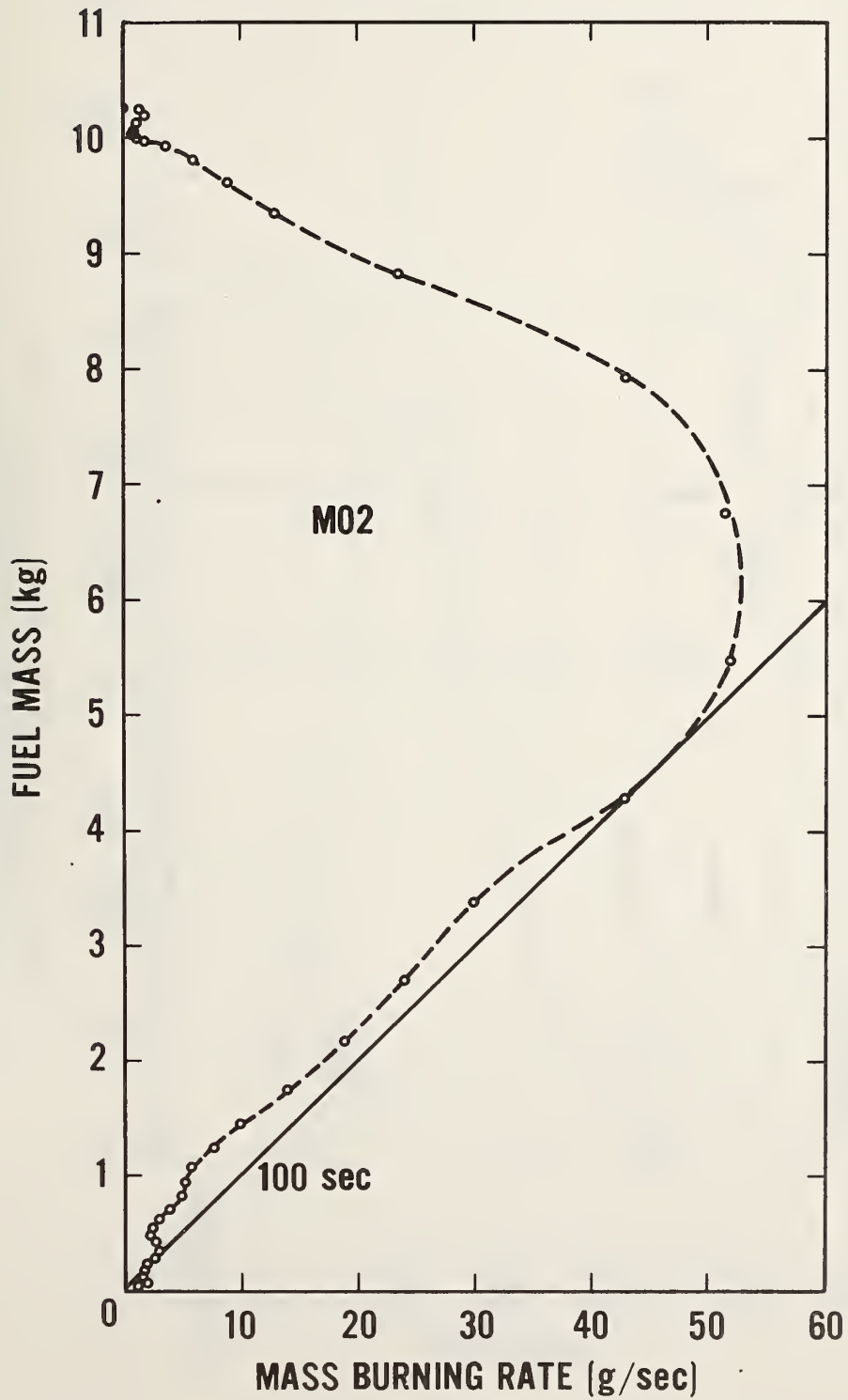




Figure 11. Remaining fuel mass plotted against mass burning rate for mattress M02. Straight line corresponds to a "late burning constant" of 100 seconds (10 g/sec/kg fuel remaining).



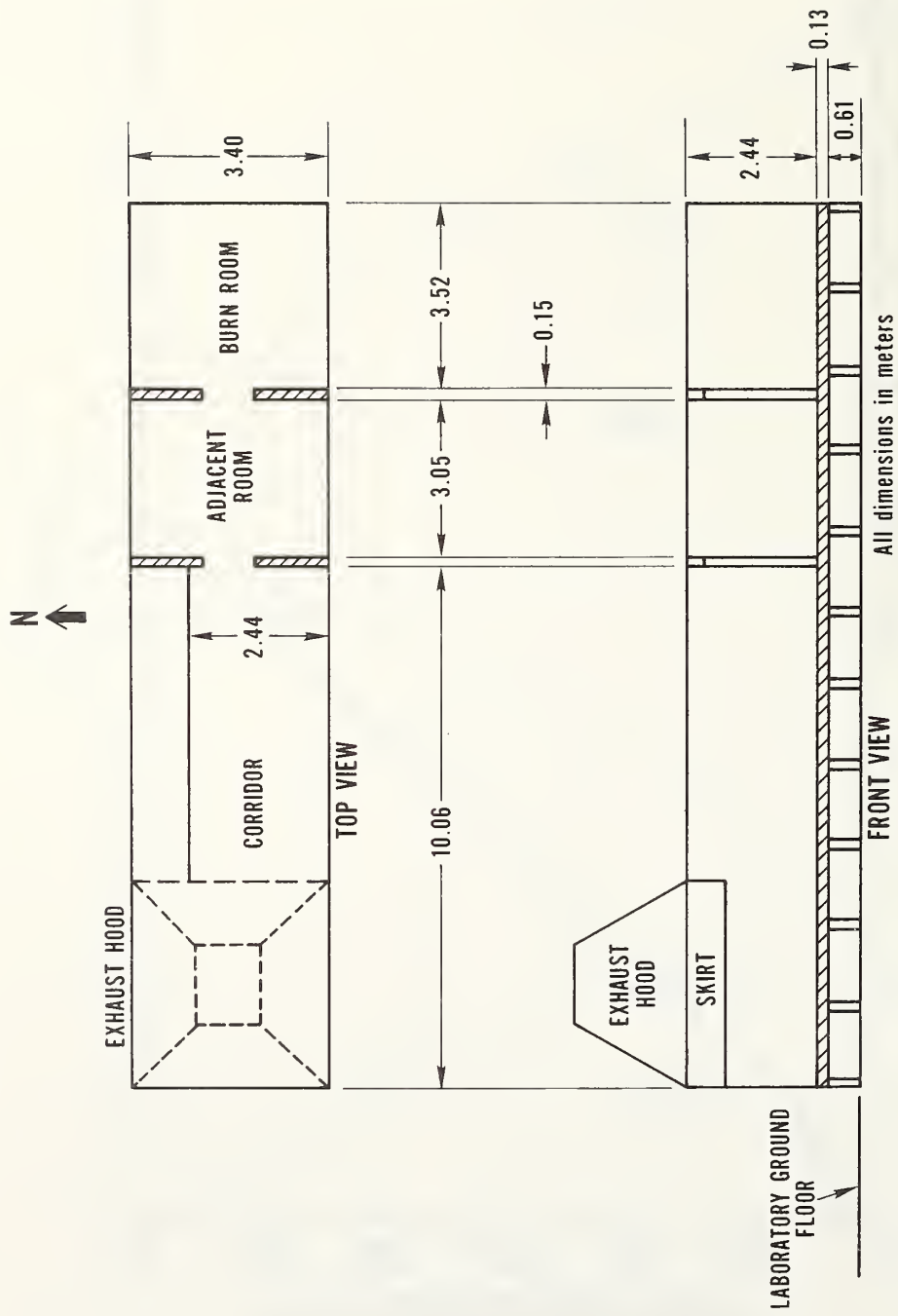
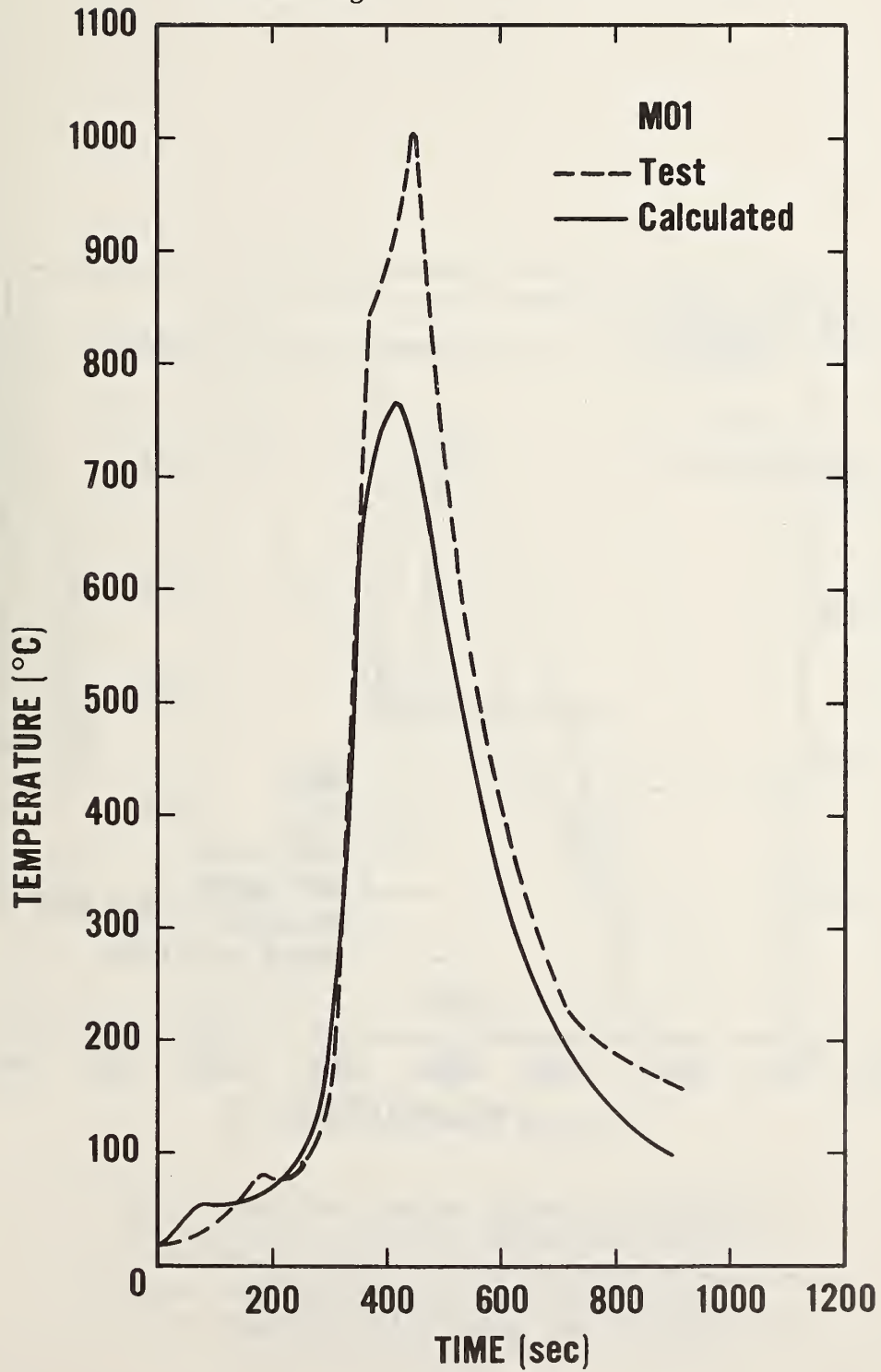


Figure 12. Location of "Room A" within the NBS Fire Test Building showing its relation to other, connecting rooms and the fire gas exhaust system.

Figure 13. Upper gas temperature versus time for mattress M01 (data from [1, figure 17]). Also shown is the calculated hot layer temperature using default values except as noted in the text. Simulation includes door mixing.



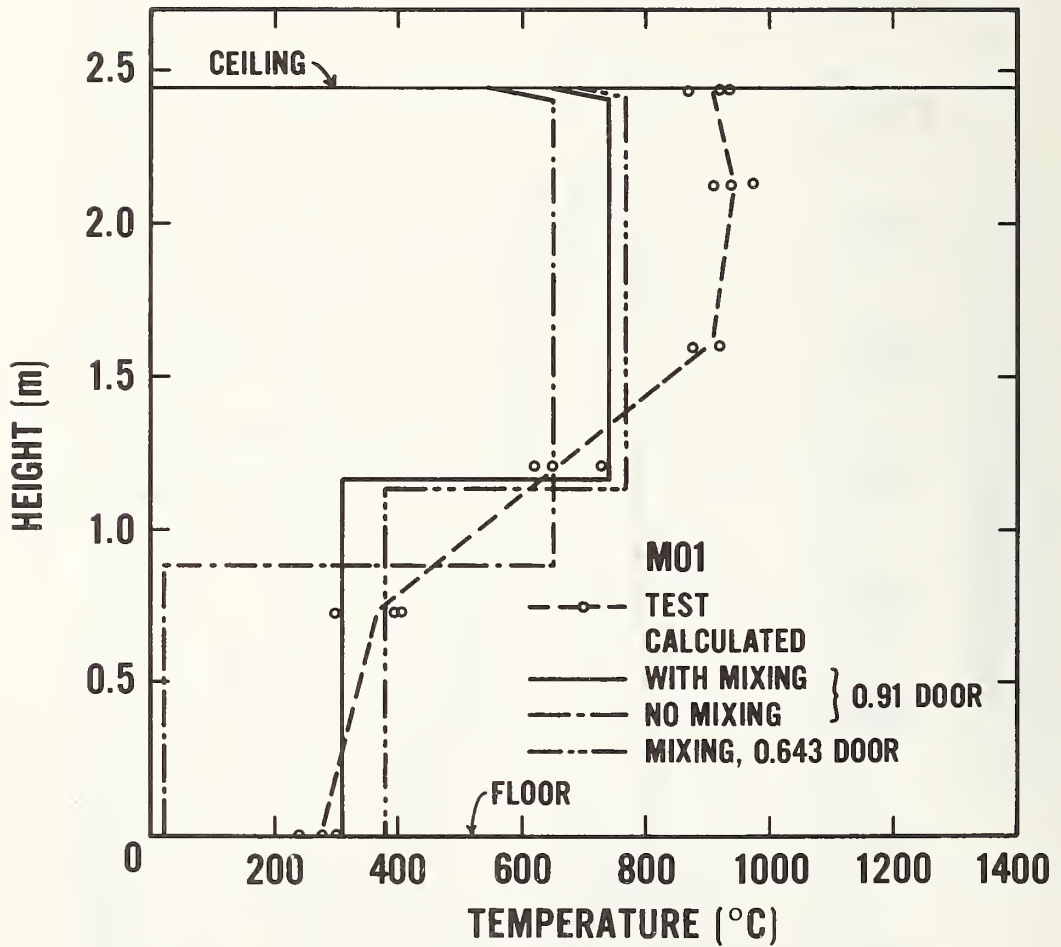


Figure 14. Height versus room temperature for mattress M01 (data from [1, fig. 23]). Also shown are the calculated vertical distribution with and without door mixing and for the door opening narrowed to 71 percent of its actual width.



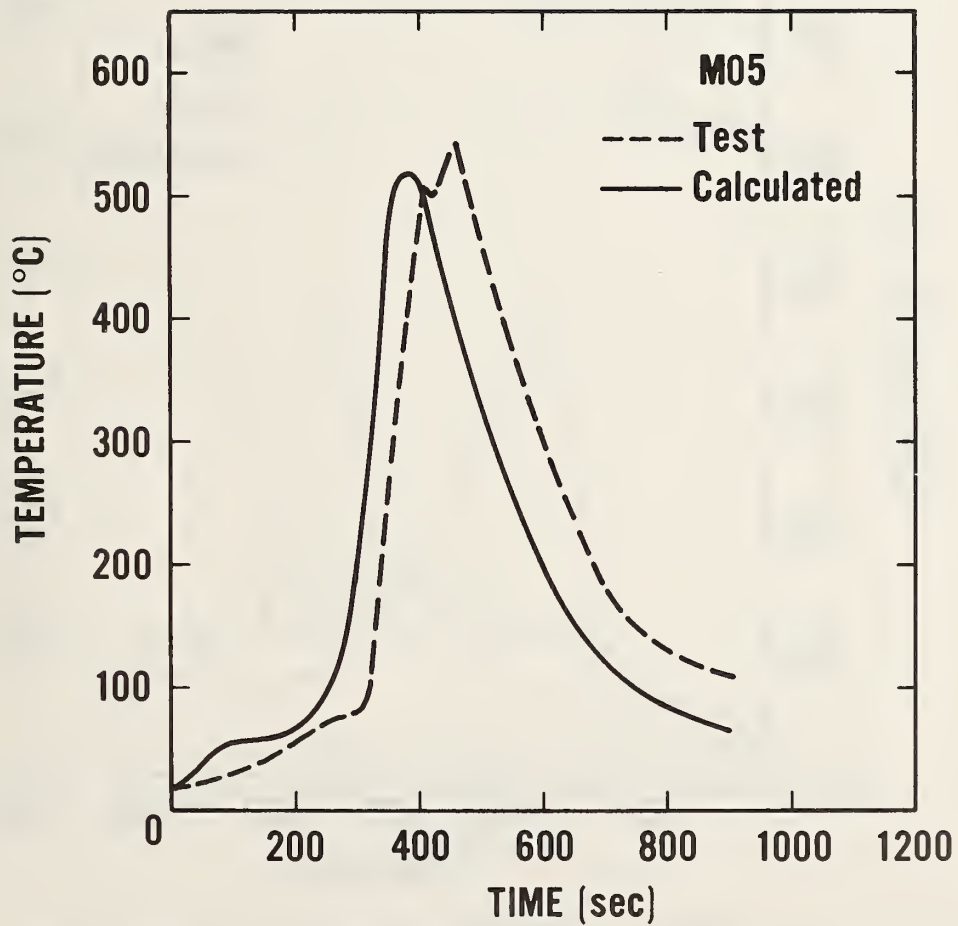


Figure 15. Upper gas temperature versus time for mattress M05 (data from [1, fig. 21]). Also shown is the calculated hot layer temperature with door mixing using Harvard default values except as noted in the text.

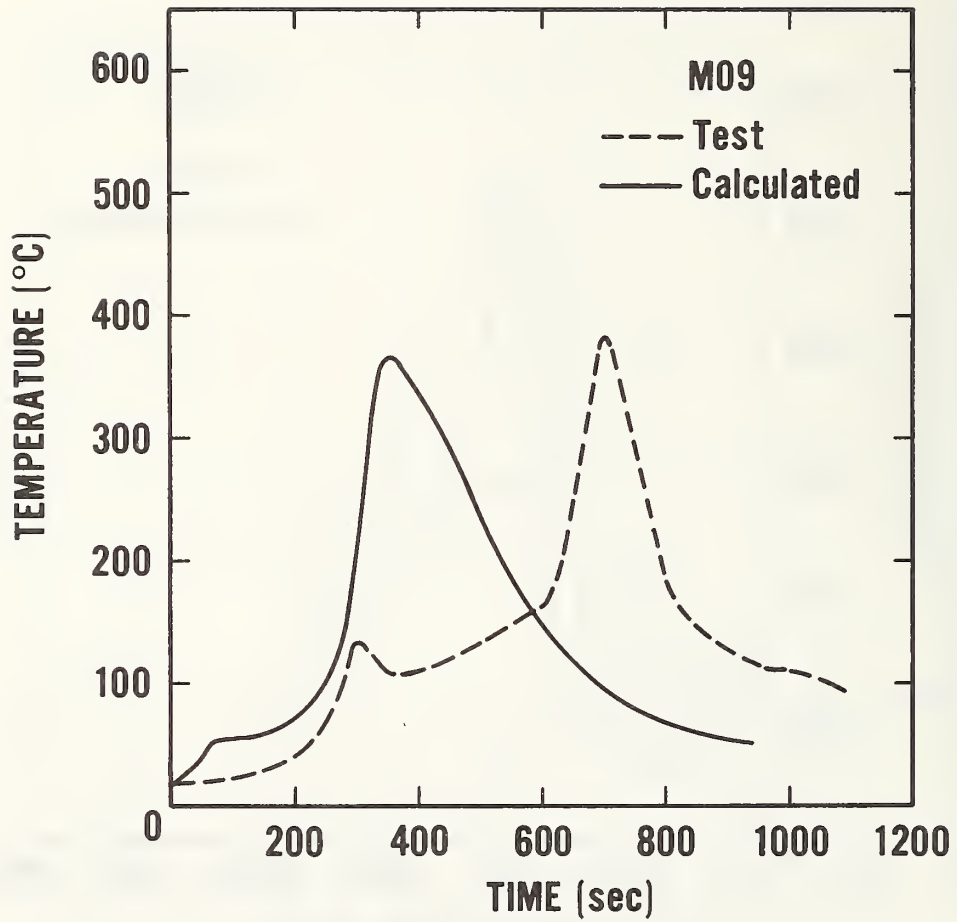


Figure 16. Upper gas temperature versus time for mattress M09 (data from [1, figure 25]). Also shown is the calculated hot layer temperature with door mixing using Harvard default values except as noted in the text.

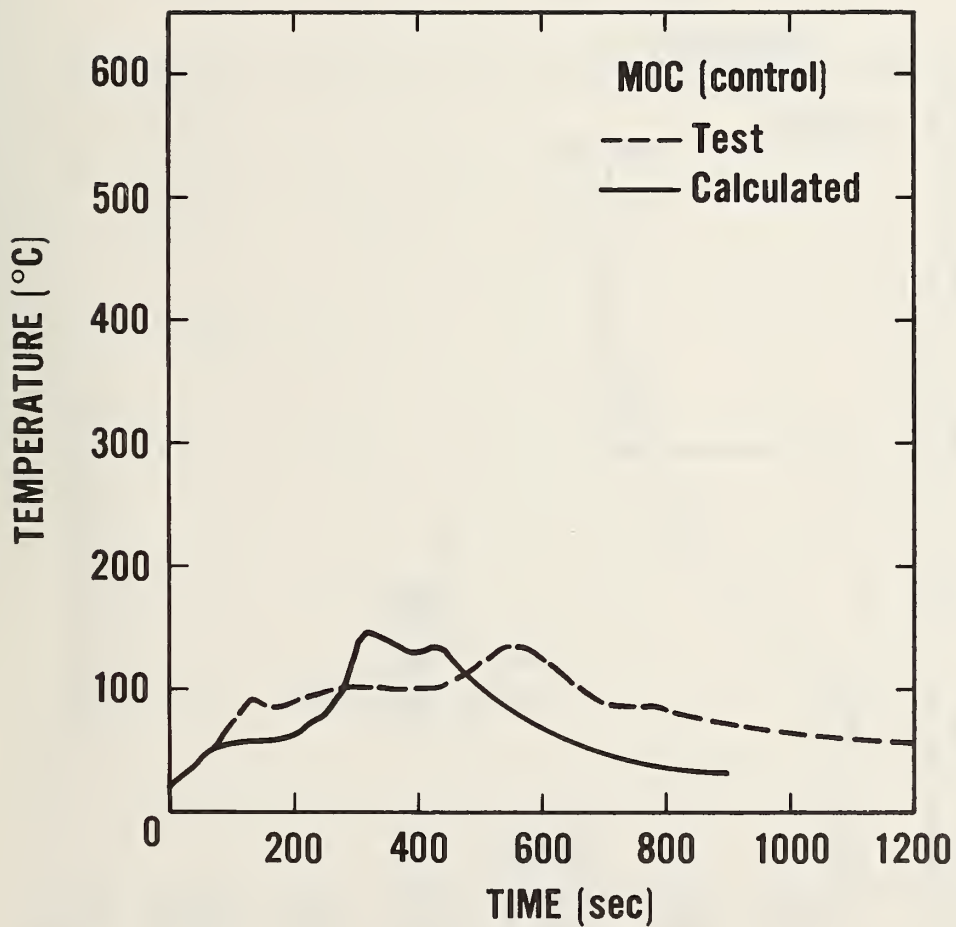


Figure 17. Upper gas temperature versus time for control mattress (data from [1, fig.16]). Also shown is the calculated hot layer temperature door mixing using Harvard default values except as noted in the text.

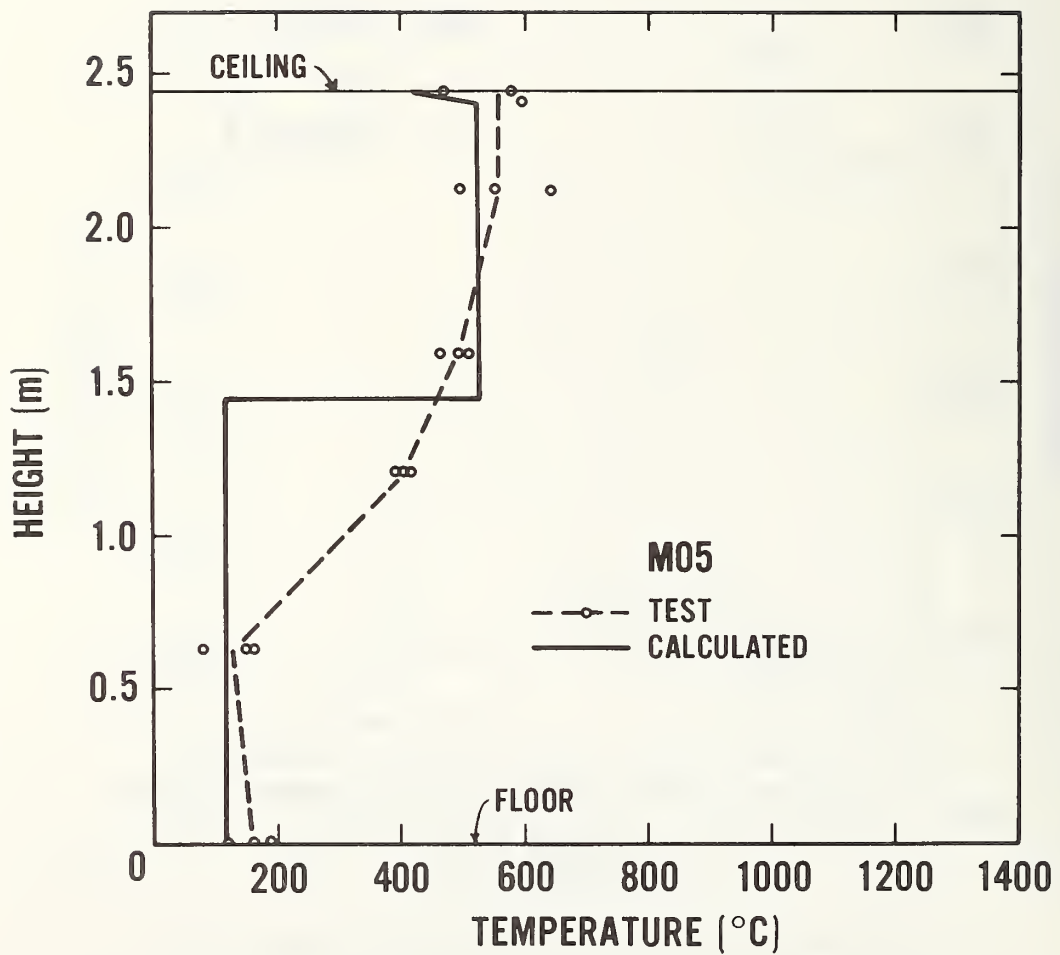
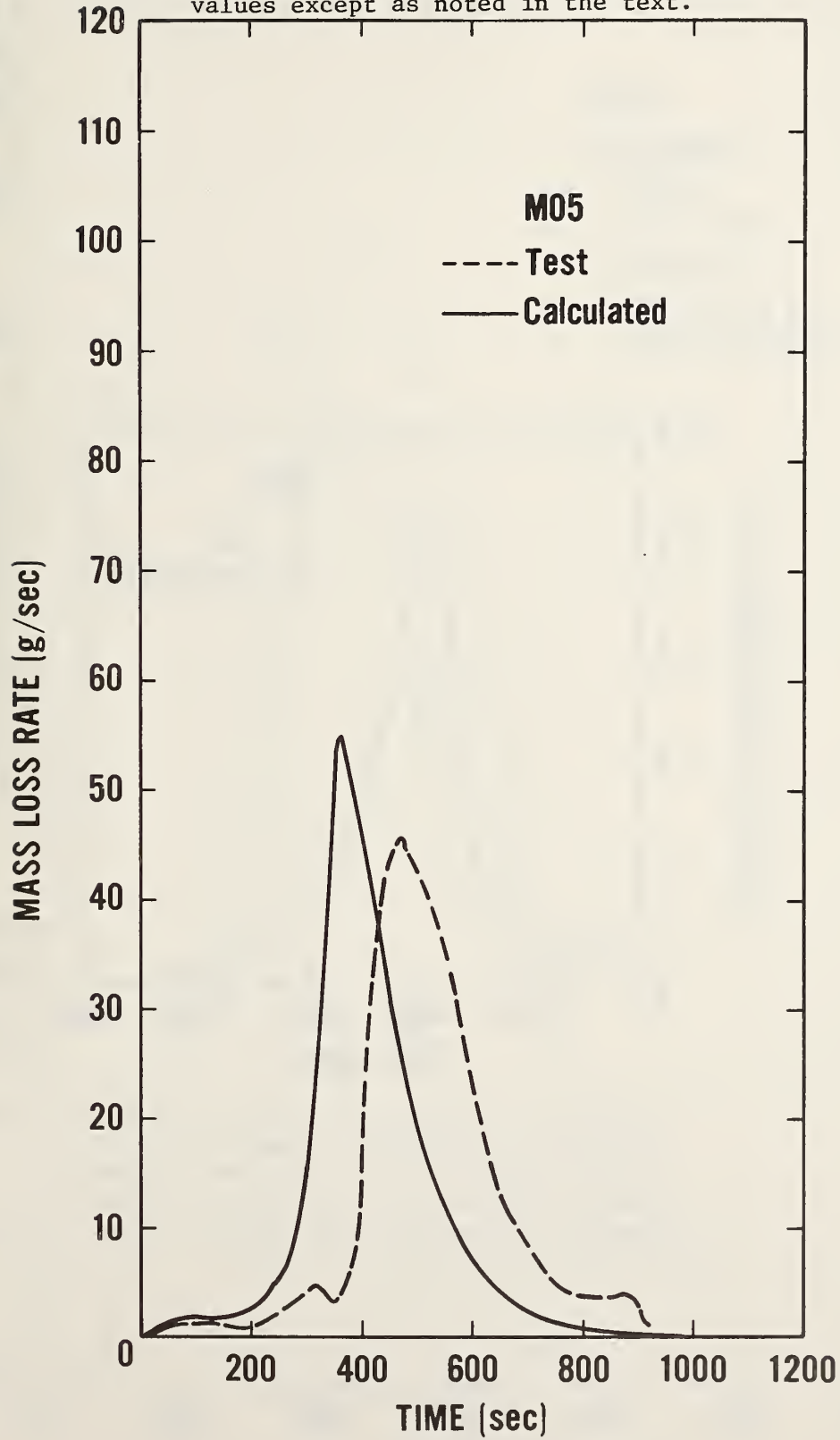


Figure 18. Height versus room temperature for mattress M05 (data from [1, fig. 32]). Also shown are the calculated vertical distribution with door mixing and door narrowed to 71 percent of actual width.

Figure 19. Mass loss rate as a function of time for mattress M05 (data from [1, figure 13]). Also shown is the calculated mass loss rate using the Harvard default values except as noted in the text.





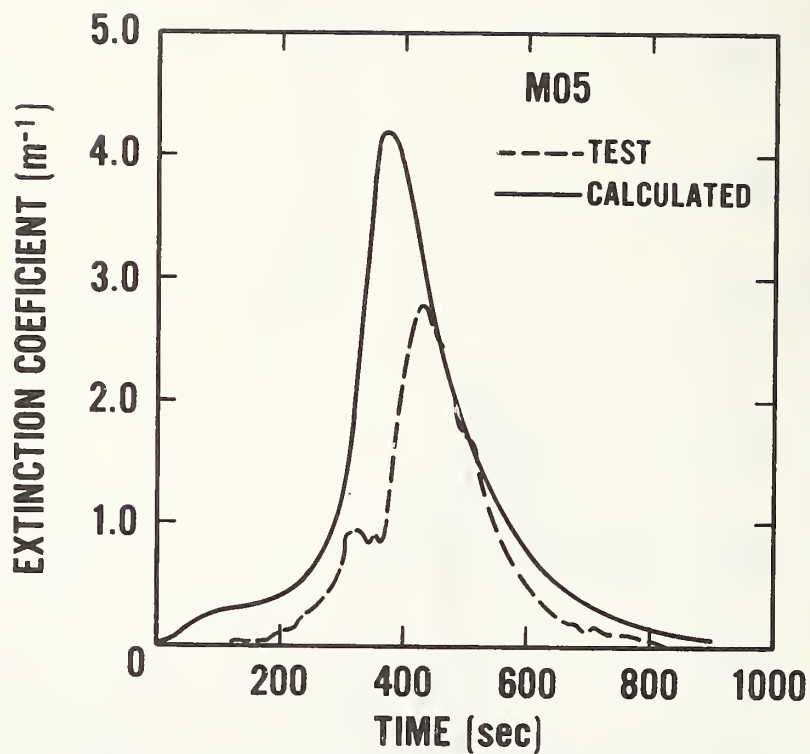
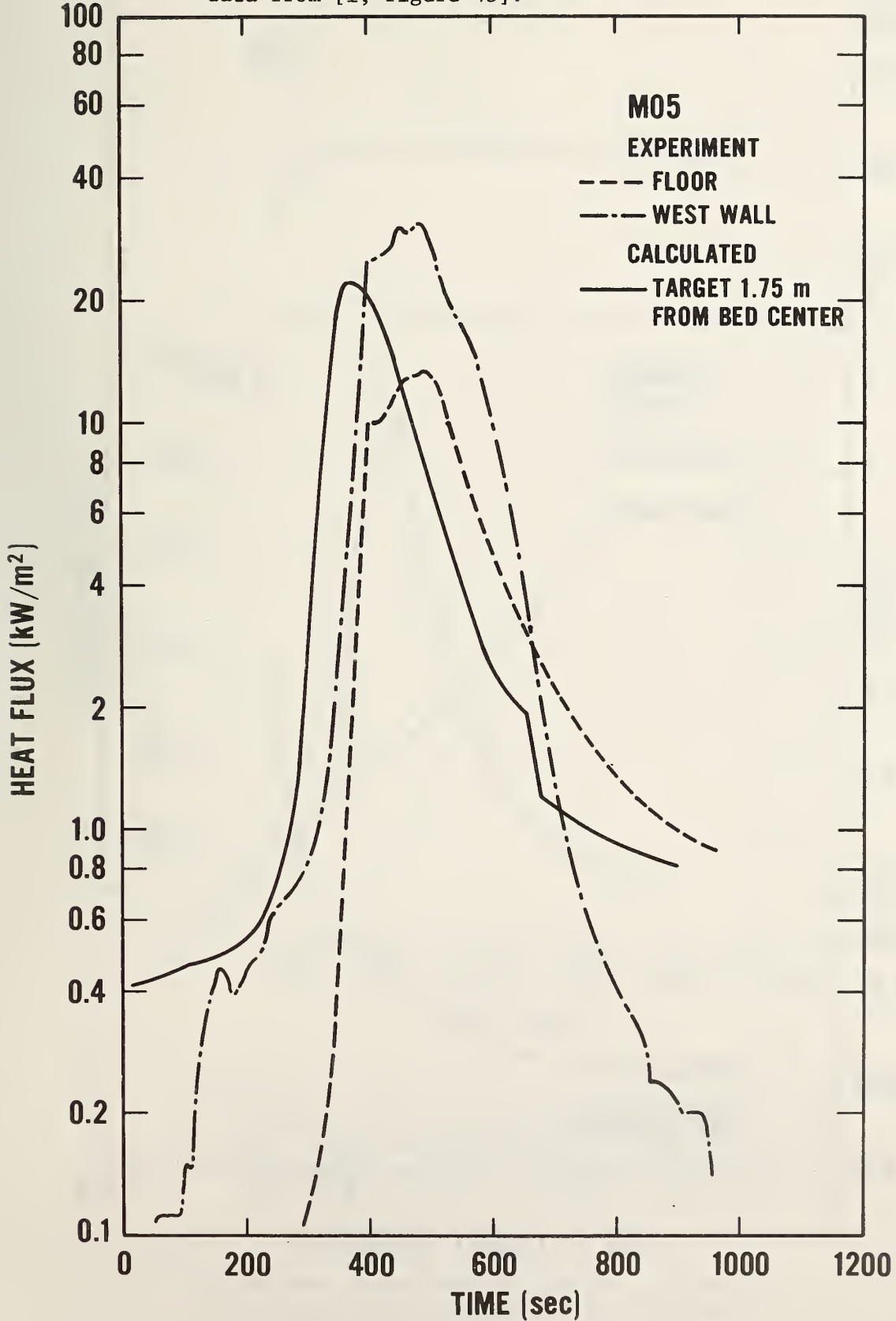


Figure 20. Extinction coefficient computed from light attenuation measurements taken in the doorway, 0.61 m below the ceiling, room A, mattress M05. Also shown is the computed extinction coefficient for the upper gas layer with  $FS = 0.241$ .

Figure 21. Comparison of measured and calculated heat flux at a target separate from the fire, mattress M05. Experimental data from [1, figure 43].



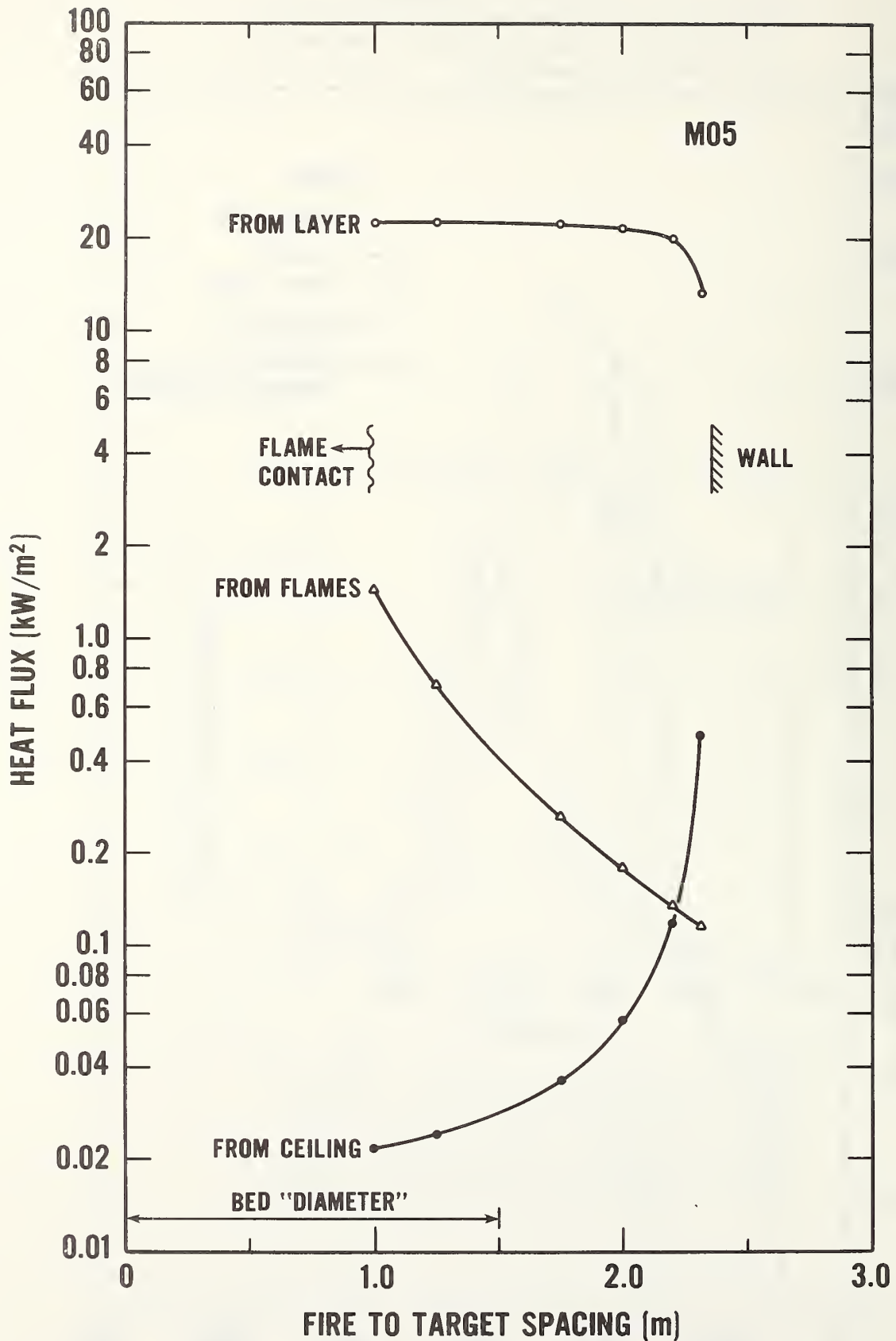


Figure 22. Effect of fire-target spacing on heat flux to the target, computed for mattress M05 at time of peak burning.

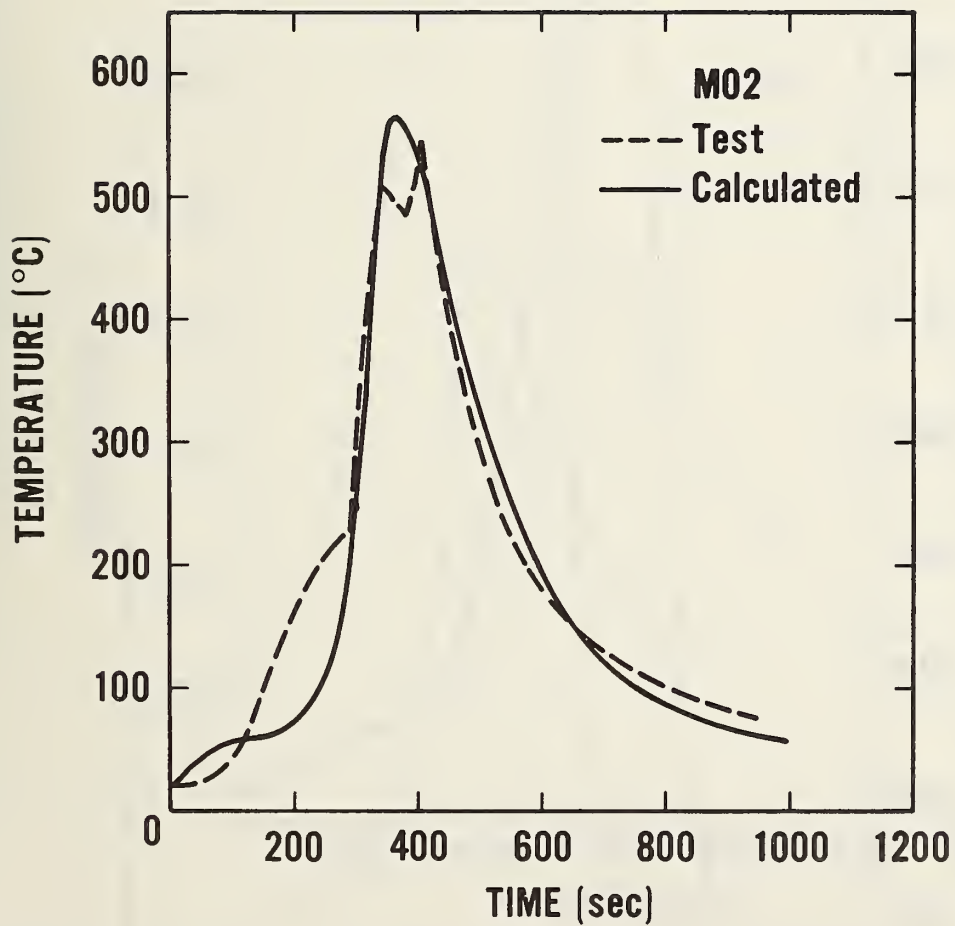


Figure 23. Upper gas temperature versus time for mattress M02 (data from [1, fig. 18]). Also shown is the calculated hot layer temperature with door mixing using Harvard Code default values except as noted in the text.

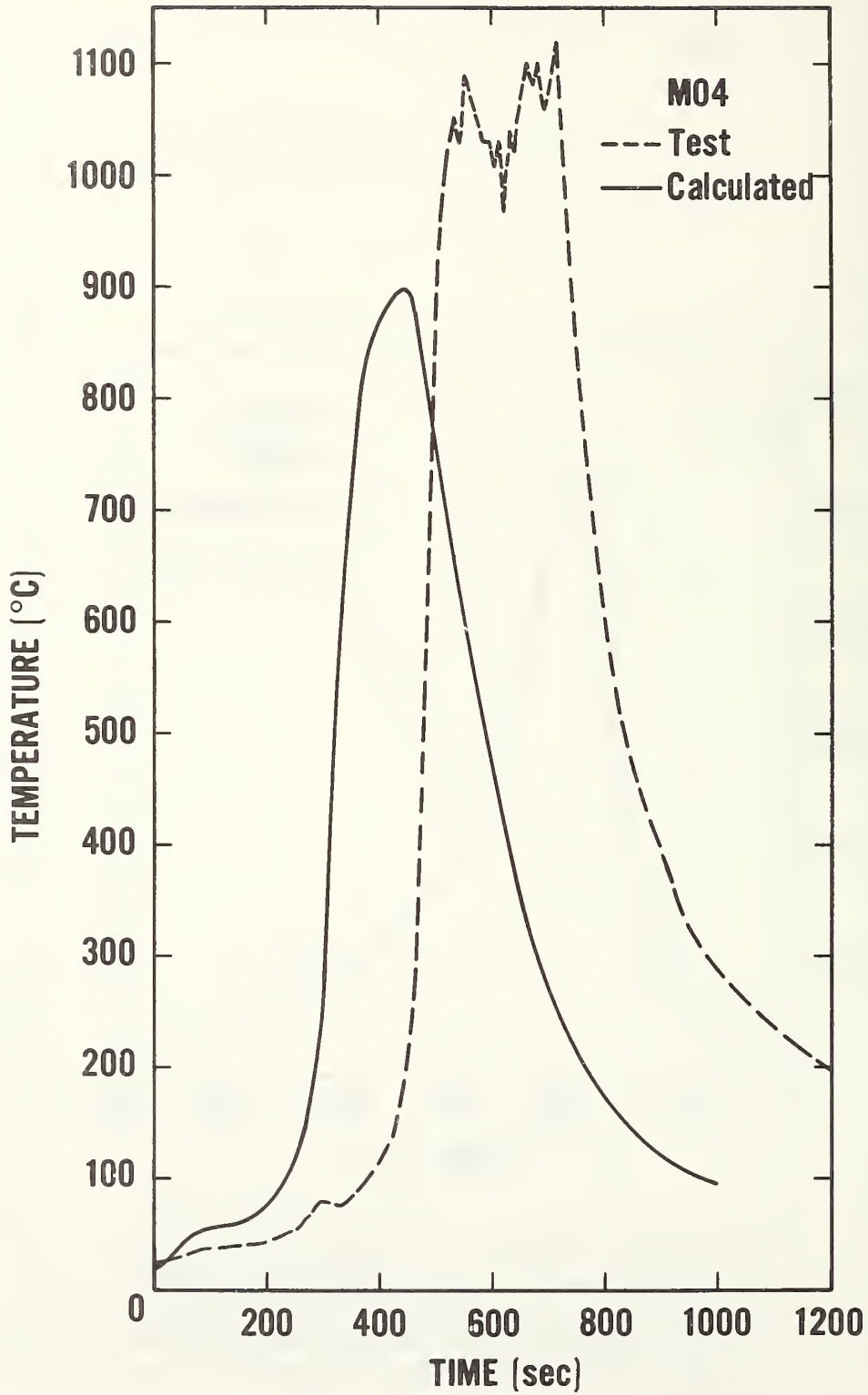


Figure 24. Upper gas temperature versus time for mattress M04 (data from [1, fig. 20]). Also shown is the calculated hot layer temperature with door mixing using Harvard default values except as noted in the text.



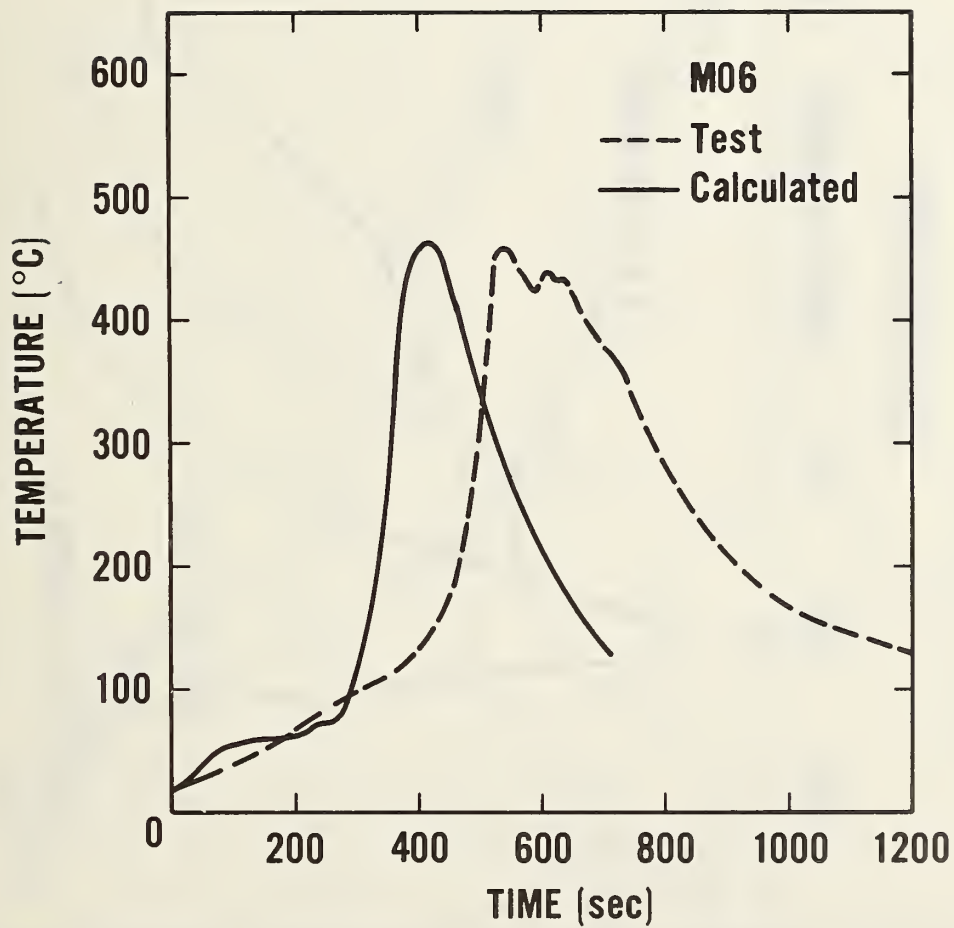


Figure 25. Upper gas temperature versus time for mattress M02 (data from [1, figure 22]). Also shown is the calculated hot layer temperature with door mixing using Harvard default values except as noted in the text.

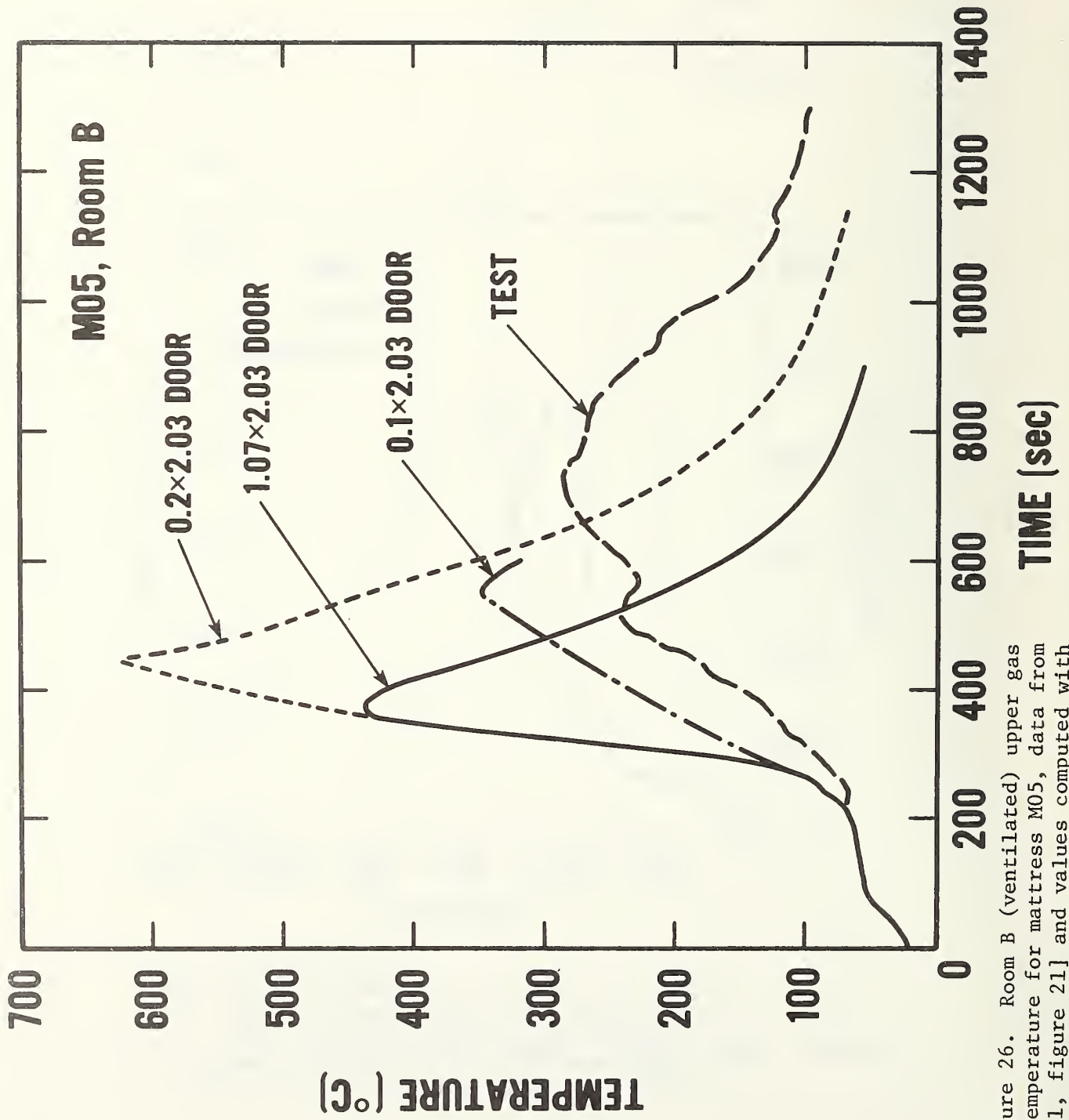


Figure 26. Room B (ventilated) upper gas temperature for mattress M05, data from [1, figure 21] and values computed with the room door fully open and closed to several widths.

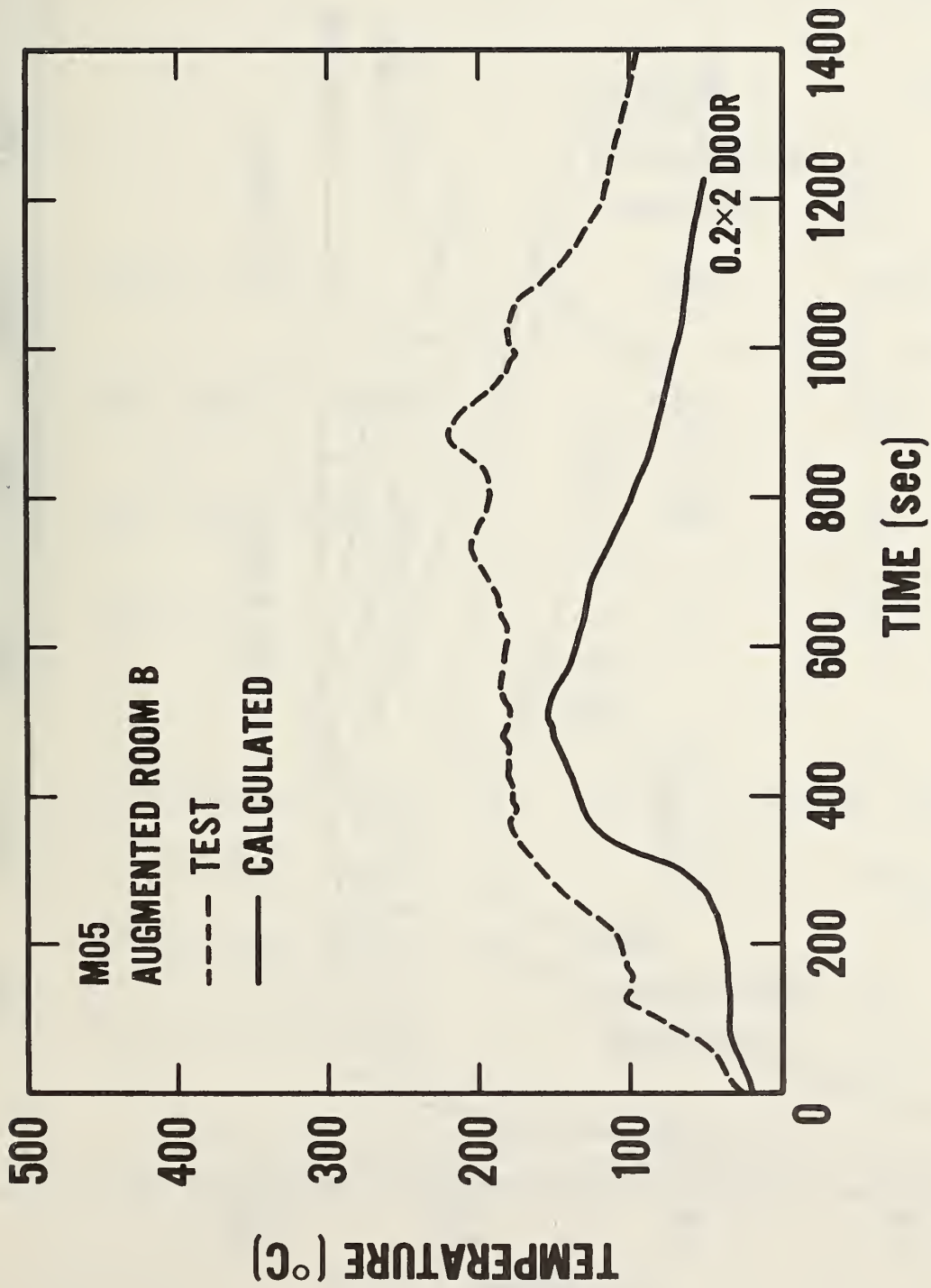


Figure 27. Room B (un-ventilated, augmented area) upper gas temperature for mattress M05 data from [1, figure 21] and values computed with the room door closed to 0.2 m width.

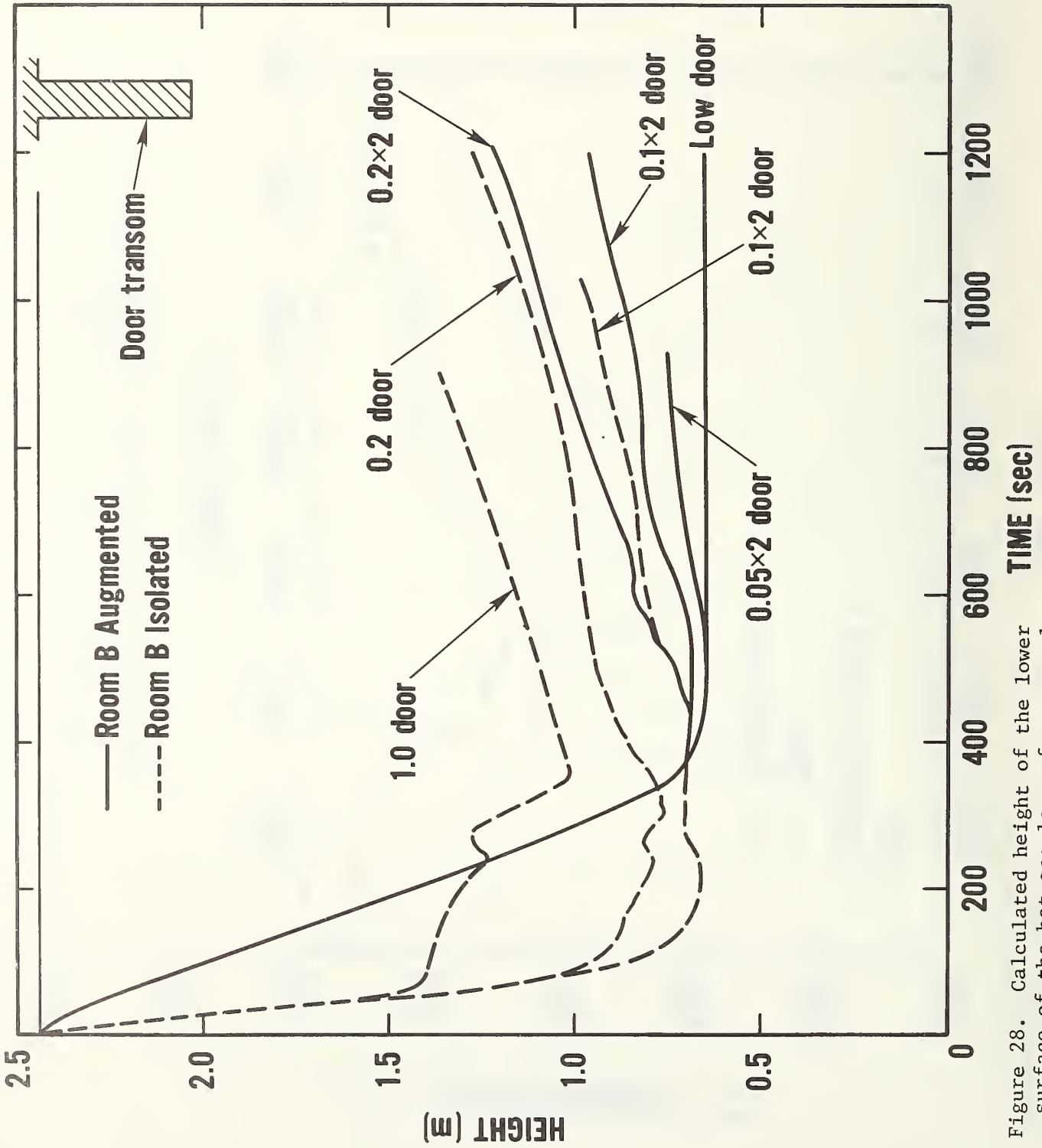


Figure 28. Calculated height of the lower surface of the hot gas layer for several cases, room B and room B (augmented).

$$I_{10} = I_3$$

$$I_{20} = e_w T_w^4 + (1 - e_w) I_1$$

$$I_{30} = e_f T_f^4 + (1 - e_f) I_4$$

$$I_{40} = I_2$$

$$I_1 = (1 - e_H) I_{10} + e_H T_H^4$$

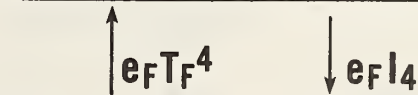
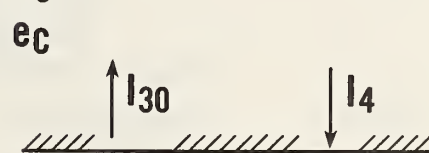
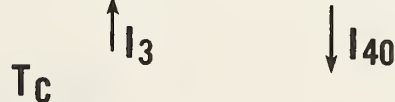
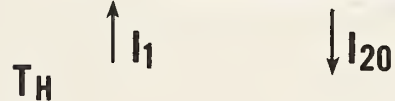
$$I_2 = (1 - e_H) I_{20} + e_H T_H^4$$

$$I_3 = (1 - e_C) I_{30} + e_C T_C^4$$

$$I_4 = (1 - e_C) I_{40} + e_C T_C^4$$

**CEILING:**

TEMPERATURE  $T_w$   
EMISSIVITY  $e_w$



**FLOOR:**

TEMPERATURE  $T_f$   
EMISSIVITY  $e_f$

Figure A2.1 Room radiative heat flux calculation showing the equations to be solved and the geometric relation of the terms.



Figure A3.1 Door mass outflow rate as a function of heat release rate. Points from Steckler [A3.1], curve calculated.

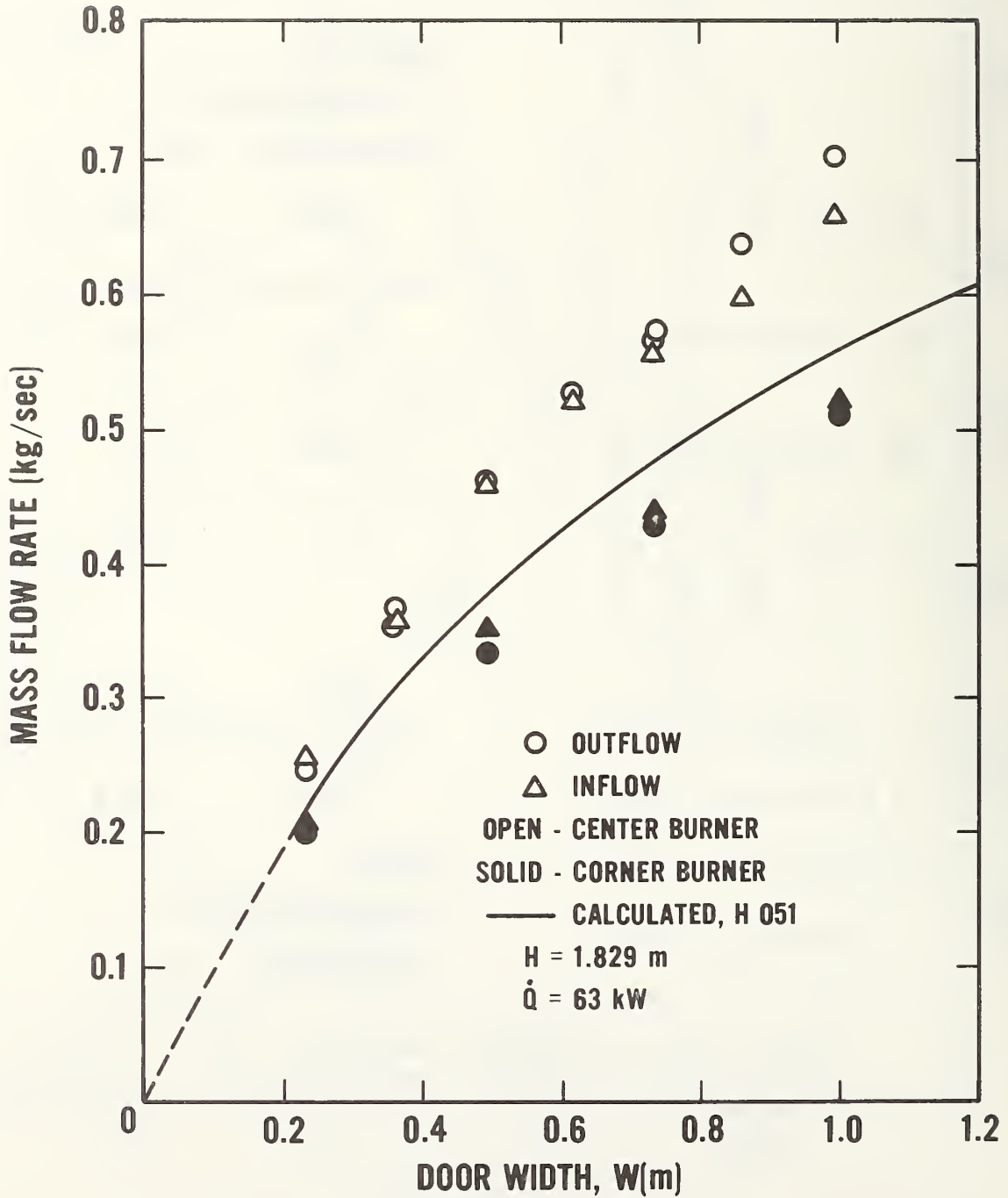
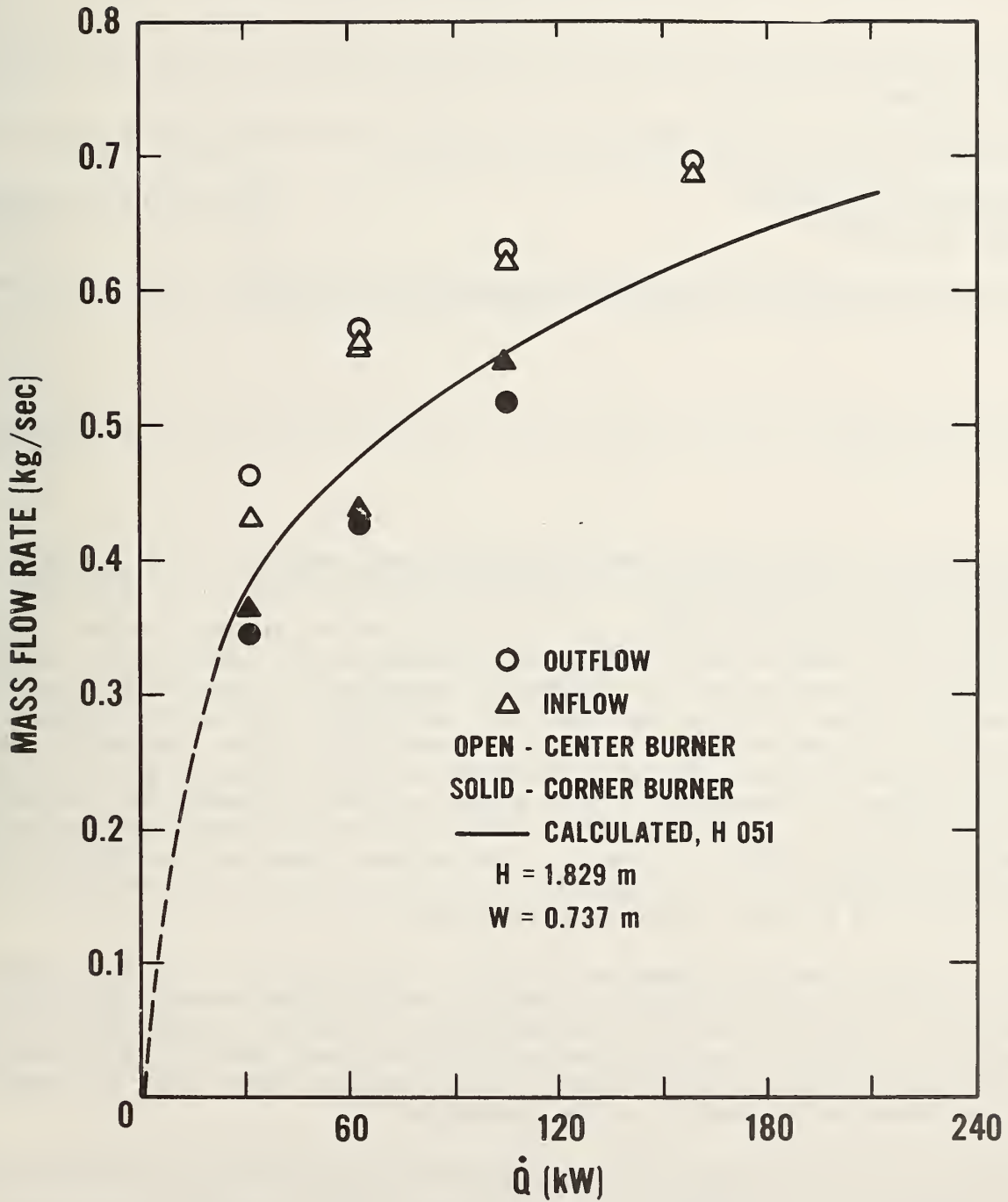


Figure A3.2 Door mass outflow rate as a function of door width. Points from Steckler [A3.1], curve calculated.



U.S. DEPT. OF COMM. <b>BIBLIOGRAPHIC DATA SHEET</b> (See instructions)	<b>1. PUBLICATION OR REPORT NO.</b> NBSIR 81-2440	<b>2. Performing Organ. Report No.</b>	<b>3. Publication Date</b> January 1982
<b>4. TITLE AND SUBTITLE</b> Modeling of NBS Mattress Tests with the Harvard Mark V Fire Simulation			
<b>5. AUTHOR(S)</b> John A. Rockett			
<b>6. PERFORMING ORGANIZATION</b> (If joint or other than NBS, see instructions) NATIONAL BUREAU OF STANDARDS DEPARTMENT OF COMMERCE WASHINGTON, D.C. 20234		<b>7. Contract/Grant No.</b>  <b>8. Type of Report &amp; Period Covered</b>	
<b>9. SPONSORING ORGANIZATION NAME AND COMPLETE ADDRESS</b> (Street, City, State, ZIP)			
<b>10. SUPPLEMENTARY NOTES</b>  <input type="checkbox"/> Document describes a computer program; SF-185, FIPS Software Summary, is attached.			
<b>11. ABSTRACT</b> (A 200-word or less factual summary of most significant information. If document includes a significant bibliography or literature survey, mention it here) NBS burned eleven mattresses made up with bedding in two different rooms, typical of a residential bedroom and a nursing home patient room, respectively. Seven of the mattresses flamed and burned vigorously, the other four were of a construction or so heavily flame inhibited that they only smoldered. The burning behavior of the seven that flamed was modeled with the Harvard Mark V fire simulation. The experimental burn behavior for tests conducted in one room was well reproduced using only total weight of combustibles, surface area and heat of combustion. Smoke production values were found to have little effect on the predicted behavior except for the smoke production itself. Fires in a second room, whose ventilation was intentionally restricted by the configuration of the adjoining space, could not be as well reproduced by the present, single room fire model.  During this study several changes were made to the simulation. The most significant change was the inclusion of mixing of the hot, exiting fire gases with the cold incoming air. As a part of this, the inter-layer radiation exchange was reformulated to include the effect of smoke contamination of the lower layer. The reformation of the radiation model had a marked effect on the predicted upper layer gas temperatures, generally improving the quality of the simulation.			
<b>12. KEY WORDS</b> (Six to twelve entries; alphabetical order; capitalize only proper names; and separate key words by semicolons) Fabric flammability; fire models; fire tests; home fires; hospitals; mattresses; nursing homes; room fires; smoldering			
<b>13. AVAILABILITY</b> <input checked="" type="checkbox"/> Unlimited <input type="checkbox"/> For Official Distribution. Do Not Release to NTIS <input type="checkbox"/> Order From Superintendent of Documents, U.S. Government Printing Office, Washington, D.C. 20402.  <input checked="" type="checkbox"/> Order From National Technical Information Service (NTIS), Springfield, VA. 22161		<b>14. NO. OF PRINTED PAGES</b> 74  <b>15. Price</b> \$9.00	



